The heterogeneous multicrew scheduling and routing problem in road restoration

Alfredo Moreno*[1], Douglas Alem[2], Michel Gendreau[3], and Pedro Munari[1]

[1]Production Engineering Department, Federal University of São Carlos, Rod. Washington Luís Km 235,, CEP 13565-905, São Carlos, Brazil

[2]University of Edinburgh Business School, Management Science and Business Economics Group, , 29 Buccleuch Place, EH89JS, Edinburgh, UK

[3]CIRRELT and Département de mathématiques et génie industriel, École Polytechnique, , Montréal, Quebec H3C 3A7, Canada

Abstract

This paper introduces the heterogeneous multicrew scheduling and routing problem (MCSRP) in road restoration. The MCSRP consists of identifying the schedule and route of heterogeneous crews that must perform the restoration of damaged nodes used in the paths to connect a source node to demand nodes in a network affected by extreme events. The objective is to minimize the accessibility time defined as the time that the demand nodes remain unconnected from the source node. The main contributions of the paper include three novel mathematical formulations that differ in the way of modeling the scheduling decisions and the synchronization of the crews, and the development of valid inequalities based on some particular properties of the problem. Additionally, we prove that the MCSRP is NP-hard. Extensive numerical experiments with randomly generated instances and a case study based on floods and landslides disasters in Rio de Janeiro, Brazil, are performed to assess the efficiency and applicability of our approach. In particular, we show that the valid inequalities significantly improve the solvability of the mathematical models. In terms of managerial implications, our results suggest that the incorporation of multiple crews helps to reduce the worst-case accessibility times across the demand nodes, thus providing more equitable solutions.

keywords: Road restoration problem; heterogeneous crew scheduling and routing; network repair; humanitarian logistics; disaster relief.

*corresponding author: alfredmorenoarteaga@gmail.com

1 Introduction

Hurricanes, floods, landslides and earthquakes are examples of natural hazards that affect millions of people every year (EM-DAT, 2019). Specifically, these types of extreme events cause disruptions in the transportation infrastructure composed of roads, bridges, tunnels, etc., impeding access to affected areas. For instance, the 2010 Haiti earthquake generated more than 30 million cubic yards of debris (Booth, 2010) from damaged infrastructure, which includes the airport, seaport and roads within the country, constraining the access of the victims to relief aid (Van Wassenhove et al., 2010). Other examples of extreme events that have significantly affected road networks, thus compromising the accessibility to affected areas, are hurricanes in the southeastern region of the United States (Rawls and Turnquist, 2010), earthquakes in China (Hu et al., 2019), and floods and landslides in Rio de Janeiro State in Brazil (Moreno et al., 2018). Inaccessible affected areas result in a lack of commodities and delays in evacuation, rescue and medical assistance activities, thus causing victim suffering and loss of life. In an attempt to provide an effective emergency response in disaster aftermath, it is essential to restate the accessibility of the affected areas, which is popularly known in humanitarian logistics as road restoration.

In general, in road restoration problems, the affected areas and the damaged components of the transportation infrastructure are represented by demand and damaged nodes, respectively. A demand node is called accessible when there exists a path connecting it with a central supply depot using only undamaged and/or repaired nodes. Consequently, to restate the accessibility of the demand nodes, a critical subset of damaged nodes must be repaired. In this context, the multicrew scheduling and routing problem (MCSRP) primarily focuses on the restoration of the critical subset of damaged nodes that are essential to emergency response operations. Multiple crews, associated with various agencies, such as civil defense, armed forces, and firefighters, are available to perform the repair operations. The crews must be assigned to repair the damaged nodes. Additionally, for each crew, the sequence in which the damaged nodes must be repaired and the route used to reach them and return to the depot must be determined.

The crews consist of workforce teams equipped with heavy machinery, dozers, excavators, light vehicles, etc., and they may not have the same equipment. For example, one crew may have dozers and excavators to remove heavy debris from a blocked road, while another may have only workers using shovels. Some crews may not have enough resources (machinery, workforce, etc.) to repair some damaged nodes. For instance, during the removal of downed trees and debris after a flood, there are potential hazards of electrocution from contact with downed power lines or tree limbs in contact with power lines (OSHA, 2019). Only crews with the appropriate knowledge and protective equipment against electrical hazards should remove such debris. Furthermore, a crew with heavy machinery may take more time to reach the damaged nodes than a crew with only light vehicles, although the former may perform a faster restoration with the help of heavy machinery. Consequently, the crews differ in the time required to repair the damaged nodes, in the travel time between nodes, and in the set of damaged nodes that they can repair. However, the consideration of multiple heterogeneous crews in the problem has been neglected in the literature because of the complexity involved in such consideration. In fact, the single crew scheduling and

routing problem (SCSRP) is challenging due to the scheduling and routing decisions that must be integrated (Maya-Duque et al., 2016; Moreno et al., 2019). In the multicrew version of the problem, an additional complexity factor is the synchronization of the crews at the damaged nodes (Akbari and Salman, 2017a,b) because these nodes cannot be traversed unless they are completely repaired, and a crew may have to wait at some damaged nodes, while another crew performs the restoration of such nodes. In fact, the MCSRP is NP-hard, as we prove in A.

The contributions of this paper to the literature are summarized as follows: (1) we define for the first time the multicrew scheduling and routing problem (MCSRP) for road restoration; (2) we develop three mixed integer programming (MIP) models that differ in the way of modeling the scheduling decisions and the synchronization of the crews; (3) we study some particular properties of the problem and derive valid inequalities based on these properties; (4) we carry out computational experiments based on a real-world case and randomly generated instances to compare the performance of the proposed formulations and the effectiveness of the valid inequalities. Regarding practical contributions, we use our models in a thorough, real-world case study of road restoration after the 2011 megadisaster of the Serrana Region in Rio de Janeiro, Brazil. Our approach consisting of models and valid inequalities enables us to derive prescriptive recommendations to the political bodies in charge of the post-disaster operations. For example, we find that the use of more crews significantly reduces the time required to recover the accessibility of the network at the same time that provides more equitable accessibility times. Additionally, the proposed approach provides good-quality solutions in reasonable computational times and can be a first step to further develop faster solution approaches and user-friendly decisions-support tools that can help decision-makers in the aftermath of disasters.

The remainder of the paper is organized as follows. Section 2 reviews the relevant background literature. Section 3 describes the heterogeneous multicrew scheduling and routing problem. Section 4 presents the MIP models, while Section 5 defines some properties and valid inequalities for the problem. Section 6 describes the instances and discusses the computational results. We close with concluding remarks in Section 7.

2 Background literature

In this section, we review the pertinent literature related to the MCSRP. The literature search was performed on a set of bibliographic databases, namely Web of Science, Scopus, and JSTOR. The keywords used for the search were the following: "road restoration", "road repair", "arc restoration", "link restoration", "network restoration", "network repair", "roadway repair", "debris clearance", "debris removal", and "debris cleanup". The keywords were selected based on recent studies on road restoration problems and on a survey of network restoration and recovery in humanitarian operations (Çelik, 2016). Additionally, a backward and forward reference search was performed. We limited the search to journal papers published in English and between years 2000 and 2020. The review is mainly focused on the application of quantitative decision making models to assist the main decisions of the MCSRP. Particularly, we prioritize studies integrating crew scheduling and routing decisions. Therefore, some related studies (Tzeng et al., 2000; Hu

and Sheu, 2013; Tuzun Aksu and Ozdamar, 2014; Çelik et al., 2015; Lorca et al., 2017; Aslan and Çelik, 2018; Sanci and Daskin, 2019) with significant contributions to the road restoration problem literature were not included in the review since they do not explicitly integrate the aforementioned decisions.

The integration of crew scheduling and routing in road restoration has been recently studied in the literature under the assumption of a single crew available to perform the repair operations and without considering the definition of relief paths. Sahin et al. (2016) developed a model to determine the order and route to visit critical nodes. The objective of the model is to minimize the total time spent to reach all the critical nodes. Berktaş et al. (2016) introduced two mathematical models with different objectives. The first model is a reformulation of the one proposed by Sahin et al. (2016). In the second model, the authors defined a new objective function that minimizes the weighted sum of visiting times using priorities for the critical nodes. Heuristic algorithms were proposed by the authors to obtain solutions quickly. Similarly, Kasaei and Salman (2016) developed two mathematical models as well as heuristic methods to find the schedule and route of a crew. The first model minimizes the total time to restore the connectivity of disconnected components of the network while the second maximizes the total components connected in a given time limit. Ajam et al. (2019) adapted the models proposed by Kasaei and Salman (2016) to minimize the latency of critical nodes, where the latency of a node is defined as the travel time from the depot to that node, including the repair time of the traversed damaged roads. The authors developed a metaheuristic based on GRASP and variable neighborhood search.

The SCSRP was recently addressed by Maya-Duque et al. (2016); Moreno et al. (2019) and Moreno et al. (2020), minimizing the weighted sum of the accessibility time of the demand nodes. Maya-Duque et al. (2016) proposed a nonlinear formulation for the SCSRP and developed a dynamic programming algorithm and a GRASP metaheuristic to solve the problem. Moreno et al. (2019) developed a branch-and-Benders-cut algorithm for the SCSRP. Additionally, the authors proposed a construction procedure followed by a local search to provide good-quality initial solutions to warm-start the branch-and-Benders-cut algorithm. Moreno et al. (2020) proposed two metaheuristics based on decomposition and one hybrid method that combine the metaheuristics with a branch-and-Benders-cut algorithm. Kim et al. (2018) defined a golden period for the repair operations. Then, they penalized the accessibility after the golden period at a higher rate. Additionally, they considered the minimization of the completion time of the repair operations. To solve this problem, the authors developed an ant colony algorithm. Shin et al. (2019) solved the problem with the same type of algorithm, considering additional relief goods distribution decisions in the SCSRP and minimizing the time of the relief distribution.

Variants of the problem have been addressed in the literature considering multiple crews. Feng and Wang (2003) integrated crew scheduling and routing decisions considering homogeneous crews. They developed a multi-objective model to maximize the total kilometers of roads repaired, to maximize the total number of lives saved, and to minimize the risk of the restoration operations. They neither address relief paths decisions nor impose that damaged nodes cannot be used before the restoration of other damaged nodes. To incorporate the latter, Yan and Shih (2007) devised a time-space network MIP model that resorts to copies of the original nodes to

represent their respective states over the time horizon. The model minimizes the completion time of the restoration. The authors considered homogeneous crews and did not consider the synchronization of the crews. Yan and Shih (2012) solved the same problem using an ant colony algorithm. Yan et al. (2014) incorporated rescheduling repair decisions into the problem. Basically, they considered that backup repair crews can be dispatched to support the regular crews when subsequent events after the primary extreme event cause new damaged nodes over the time horizon. Tang et al. (2009) incorporated both stochastic travel and repair times into the problem using a two-stage stochastic programming model, while Yan and Shih (2009) integrated relief distribution decisions to minimize the total time of the distribution together with the completion time of the restoration. Xu and Song (2015) integrated relief distribution as well, but they focused on minimizing the time at which relief goods arrive at the demand nodes.

Özdamar et al. (2014) proposed a recursive model to schedule a fleet of homogeneous dozers that perform the task of debris cleanup from blocked arcs. They did not consider the definition of relief paths or the synchronization of the dozers. Akbari and Salman (2017a) and Akbari and Salman (2017b) introduced the synchronization of crews to recover the connectivity of a network affected by extreme events, but without integrating the definition of relief paths. Akbari and Salman (2017b) proposed an MIP model to determine the set of affected roads that need to be repaired and the synchronized routes for multiple homogeneous crews. The objective was to minimize the completion time of the restoration. However, they could not solve practical-sized instances by using the exact mathematical model. Therefore, they relaxed the problem to obtain unsynchronized solutions that are later synchronized by a heuristic. The same problem was addressed by Akbari and Salman (2017a) with a different objective function consisting of maximizing the network components connected to the depot node. Morshedlou et al. (2018) also considered multiple homogeneous crews and focused on the restoration of gas, water, and electrical power infrastructure networks, assuming that no disruption affects the transportation network. Thus, the crews do not have to wait for the restoration of damaged nodes to traverse the arcs in the road network. In this sense, the authors did not consider the synchronization of crews as defined in this paper. Furthermore, they did not define relief paths between the depot and the demand nodes.

Table 1 summarizes the main decisions, characteristic and objective functions of the most related problems considered in the literature. Although previous studies have obtained satisfactory results for the SCSRP (Maya-Duque et al., 2016; Kim et al., 2018; Shin et al., 2019; Moreno et al., 2019, 2020), their models and solution methods cannot be applied to the MCSRP. In the MCSRP, the synchronization of the crews requires the explicit definition of the arrival and waiting time of the crews at the damaged nodes, making the problem harder since the different crews can traverse a damaged node multiple times. In the SCSRP, the waiting time at the damaged nodes does not exist, and when the crew arrives at a damaged node, the crew must repair it if the node has not yet been repaired, or traverse it without waiting if the node has already been repaired. Thus, the solution methods for the SCSRP were developed without explicitly considering the arrival and waiting times of the crews at the damaged nodes, but only the time at which such nodes are repaired.

Regarding the variants of the problem considering multiple crews, we notice that there is a lack of studies considering heterogeneous crews in road restoration problems. In practice, the crews are workforce teams associated with various governmental and non-governmental agencies and may not have the same equipment to repair the damaged nodes. However, this heterogeneity has been neglected in the literature. Furthermore, most works that considered homogeneous crews lack synchronization constraints that are inherent to the problem. In fact, only two of the reviewed studies (Akbari and Salman, 2017b,a) addressed the synchronization of homogeneous crews. These authors defined the scheduling and routing of crews to visit critical nodes. Differently from the MCSRP, such critical nodes are defined a priori and do not necessarily represent damaged nodes. Furthermore, they did not integrate decisions related to the definition of the relief paths connecting the source node with the demand nodes. In the MCSRP, the consideration of such paths is important because they define the critically damaged nodes that must be immediately repaired to perform emergency response. In this paper, we help to fill these gaps by proposing mathematical formulations and valid inequalities for the MCSRP with synchronized heterogeneous crews.

Table 1: Main characteristics, objective functions and decisions of the reviewed literature.

	Characteristics		Objective functions				Main decisions				
Reference	Multi-crew[1]	Synchro-nization	Accessibi-lity time	Comple-tion time	Distri-tion time	Other[2]	Assign-ment	Sche-duling	Rou-ting	Relief path	Distri-bution
Sahin et al. (2016)	S			✓				✓	✓		
Berktaş et al. (2016)	S			✓		✓		✓	✓		
Kasaei and Salman (2016)	S		✓			✓		✓	✓		
Maya-Duque et al. (2016)	S		✓					✓	✓	✓	
Kim et al. (2018)	S		✓	✓				✓	✓	✓	
Moreno et al. (2019)	S		✓					✓	✓	✓	
Moreno et al. (2020)	S		✓					✓	✓	✓	
Shin et al. (2019)	S				✓			✓	✓	✓	✓
Ajam et al. (2019)	S					✓		✓	✓		
Feng and Wang (2003)	M-Hm					✓	✓	✓	✓		
Yan and Shih (2007)	M-Hm			✓			✓	✓	✓		
Yan and Shih (2009)	M-Hm			✓	✓		✓	✓	✓	✓	✓
Tang et al. (2009)	M-Hm			✓		✓	✓	✓	✓		
Yan and Shih (2012)	M-Hm			✓			✓	✓	✓		
Özdamar et al. (2014)	M-Hm			✓		✓	✓	✓	✓		
Yan et al. (2014)	M-Hm			✓			✓	✓	✓		
Xu and Song (2015)	M-Hm				✓		✓	✓	✓	✓	✓
Akbari and Salman (2017b)	M-Hm	✓		✓			✓	✓	✓		
Akbari and Salman (2017a)	M-Hm	✓				✓	✓	✓	✓		
Morshedlou et al. (2018)	M-Hm					✓	✓	✓	✓		
This paper	M-Ht	✓	✓				✓	✓	✓	✓	

[1] S: single crew; M-Hm: homogeneous multi-crew; M-Ht: heterogeneous multi-crew.
[2] Visiting time; number of components connected; latency; length of road open; risk; number of life savings; network inaccessibility; resilience.

3 Problem description

The *multicrew scheduling and routing problem* (MCSRP) is defined on an undirected graph $G = (\mathcal{V}, E)$, in which $\mathcal{V}$ is the set of nodes, and E is the set of undirected arcs. The subset $\mathcal{V}^{\mathtt{d}} \subset \mathcal{V}$ characterizes the demand nodes, while the subset $\mathcal{V}^{\mathtt{r}} \subset \mathcal{V}$ contains the collection of damaged nodes. Furthermore, there may be intersection nodes that represent the intersection of two or more arcs. There is one depot (node 0) that is a supply node to be connected to the demand nodes. Figure 1(a) shows an illustrative example of a graph G representing a damaged network composed of two municipalities (Nova Friburgo and Teresópolis) and four damaged nodes located on four highways (RJ-116, RJ-122, RJ-130 and RJ-142).

A set $\mathcal{K}$ of multiple heterogeneous crews is available to perform the restoration activities. The crews are initially located in the central depot and differ in the time required to repair the damaged nodes (δ_{ki}), in the travel time on the arcs (τ_{ke}), and in the set of damaged nodes that each crew can repair. We assume that travel and repair times can be estimated by collecting post-disaster information on road conditions. This data can be provided by various tools such as satellite images, geographic information systems or drones (Akbari and Salman, 2017a,b). Basically, the MCSRP consists of determining (i) the paths to connect the depot to the demand nodes (relief path decisions), (ii) the assignment of crews to the damaged nodes (assignment decisions), (iii) the schedule of crews to repair the damaged nodes (scheduling decisions), and (iv) the routes of crews to repair the damaged nodes and return to the depot (routing decisions). Figure 1(b) illustrates the main decisions attributed to the MCSRP, highlighting the schedule of two crews (red arrows), the route of a crew (black arrows), and one relief path (green arrows). The scheduling decision includes the assignment of crews to damaged nodes.

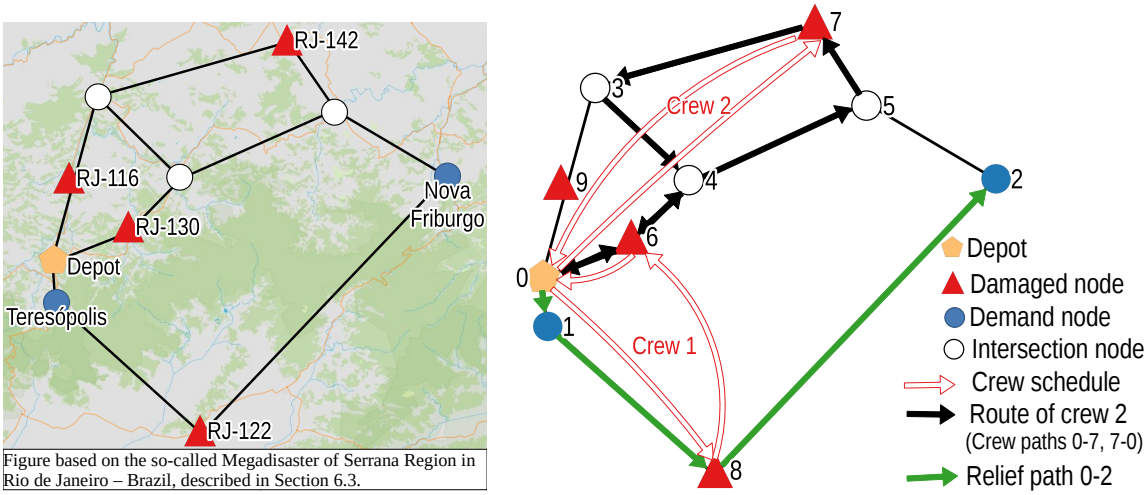

(a) Graph G. (b) Decisions attributed to the MCSRP.

Figure 1: Example of a graph G and decisions attributed to the MCSRP.

The relief path decision defines the sequence of nodes and arcs used to connect the depot with the demand nodes to perform the distribution, evacuation and/or rescue operations. A given relief path connecting the depot with the demand node i is called a relief path $0-i$. For instance, Figure 1(b) shows an example of a relief path $0-2$ (green arrows), which is defined by the sequence of nodes $0 \rightarrow 1 \rightarrow 8 \rightarrow 2$. Multiple paths may be available to reach a given demand node i. For example, the sequence $0 \rightarrow 6 \rightarrow 4 \rightarrow 5 \rightarrow 2$ is an alternative relief path $0-2$. The total distance of a relief path $0-i$ must be less than or equal to a predefined maximum distance l_i^{d}. Tight values for l_i^{d} might help to avoid the selection of long relief paths in terms of distance. It is also possible to set l_i^{d} to a sufficiently large number so as to allow the selection of relief paths of any length. The damaged nodes used in the relief paths must be repaired by the available crews as soon as possible to minimize the time that the demand nodes remain inaccessible from the depot (accessibility time). A demand node $i \in \mathcal{V}^{\mathrm{d}}$ is called accessible if there exists a relief path $0-i$ using only undamaged and/or repaired nodes. Thus, the accessibility time of demand

node i depends on the time at which the damaged nodes used in relief path $0-i$ are repaired. In Figure 1(b), for example, demand node 2 becomes accessible after the restoration of damaged node 8. When no damaged nodes are used in a relief path $0-i$, the corresponding accessibility time of demand node i is zero.

The assignment decision determines the damaged nodes that need to be repaired, and the crew that must perform their restoration. The scheduling decisions define, for each crew, the repair order of the damaged nodes. Figure 1(b) shows the assignment and scheduling decisions for two crews (red arrows). Crew 1 is assigned to repair damaged nodes 6 and 8, while crew 2 must perform the restoration of damaged node 7. The schedule for the first crew is defined by the ordered set of nodes (0, 8, 6, 0). Thus, node 8 is repaired before node 6. Since the crews must depart and return to the depot, we include node 0 at the beginning and at the end of each schedule. The assignments and schedules defined for the crews may not need to include all the damaged nodes. A subset of damaged nodes may be enough to make the demand nodes accessible. For example, only damaged node 8 needs to be repaired to enable relief path $0-2$. However, solutions repairing more than the needed damaged nodes are feasible for the problem.

The routing decisions determine the paths/routes to be used by the crews to repair the damaged nodes and return to the depot. A path associated with a given crew is a sequence of nodes and arcs used by this crew to travel between two consecutive damaged nodes in its schedule. A path used by a crew to travel from node i to node j is called crew path $i-j$. Crew path $0-7$ in Figure 1(b) is defined by the sequence of nodes $0 \rightarrow 6 \rightarrow 4 \rightarrow 5 \rightarrow 7$, while crew path $7-0$ is defined by the sequence of nodes $7 \rightarrow 3 \rightarrow 4 \rightarrow 6 \rightarrow 0$. More than one path can be available for a crew to travel from one damaged node to the next in its schedule. For example, the path defined by nodes $0 \rightarrow 1 \rightarrow 8 \rightarrow 2 \rightarrow 5 \rightarrow 7$ is an alternative crew path $0-7$. For a given crew, a route is a sequence of paths that ends at the depot after repairing all the damaged nodes in its schedule. The route for crew 2 consists of crew paths $0-7$ and $7-0$. Nodes and edges can be traversed multiple times by the crews. A damaged node i is repaired when it is visited for the first time by crew k assigned to its restoration. In this case, crew k incurs in the repair time δ_{ki}. The crews can use the already repaired damaged nodes multiple times after their restoration without incurring extra repair time. Some damaged nodes cannot be accessed directly from the depot without the restoration of other intermediate damaged nodes. This is the case for node 7 in Figure 1(b), for example. The time spent by a given crew to return to the depot after repairing all the damaged nodes in its schedule does not affect the accessibility time of the demand nodes. Therefore, any feasible path composed of repaired damaged nodes and/or undamaged nodes can be used by the crews to return to the depot without affecting the value of the objective function. In Figure 1(b), for example, the time spent by crew 1 to return to the depot using the crew path $6-0$ does not affect the accessibility time since the last damaged node in its schedule (node 6) has been already repaired.

It is assumed that the same crew cannot restore more than one damaged node simultaneously, and damaged nodes cannot be repaired by more than one crew. As a consequence of the latter assumption, if a given crew reaches a damaged node that is already being repaired, then this crew has to wait until the damaged node is totally repaired. This reflects the practical situations

in which the limited space or other adverse conditions sometimes prevent the use of more than one crew to perform simultaneously the restoration of a same damaged node. For example, it is difficult for two or more dozers (crews) to act over a landslide in a narrow road or when the ground remains unstable after the landslide. Given the schedules presented in Figure 1, crew 2 could have to wait to cross damaged node 6, which is repaired by crew 1. In this case, the time at which crew 2 can cross node 6 must be synchronized with the time at which crew 1 completes the restoration of this node. Alternative solutions for the problem could not require the synchronization of the crews. This is the case, for example, if crew 2 repairs by itself the damaged node 6 or if crew 2 uses an alternative path to avoid crossing damaged node 6. In fact, the waiting time of a crew in a given damaged node i is necessary only if there is not a faster crew path available.

Different from the single crew version of the problem, the synchronization of crews in the MCSRP requires the consideration of both the arrival and waiting times at each damaged node crossed in the paths of the crews. This increases the difficulty of the problem in terms of tractability of the MIP model representing the MCSRP with respect to the SCSRP given the number of additional variables and constraints that must be considered. Nevertheless, neglecting the synchronization in the MCSRP can significantly deteriorate the solutions to the problem. For instance, consider the schedules presented in Figure 1(b) and assume that crew 1 completes the restoration of nodes 8 and 6 after 2 and 4 hours, respectively. Additionally, assume that the travel time of crew 2 is 1 hour for all arcs. Figure 2 shows two possible paths for crew 2 to travel from node 0 to damaged node 7 with and without considering the synchronization of the crews. Path 1 is defined by nodes $0 \rightarrow 6 \rightarrow 4 \rightarrow 5 \rightarrow 7$, while path 2 is defined by nodes $0 \rightarrow 1 \rightarrow 8 \rightarrow 2 \rightarrow 5 \rightarrow 7$. When the synchronization is neglected, we assume that the damaged nodes visited in paths 1 and 2 can be used without incurring waiting time. In this case, the best path for arriving at damaged node 7 seems to be path 1, and crew 2 arrives at node 7 after 4 hours. However, when we consider the synchronization of the crews, crew 2 has a waiting time of 3 hours using path 1 because damaged node 6 can be crossed only after 4 hours. Then, using path 1 implies crew 2 arrives at node 7 after 7 hours and not after 4 hours as was wrongly determined when no waiting time was considered. In contrast, path 2 has no waiting time since damaged node 8 is already repaired when crew 2 arrives. Therefore, ignoring the synchronization implies neglecting the waiting time, which in turn leads to the selection of path 1. This strategy delays the restoration of damaged node 7 by 2 hours with respect to the selection of path 2.

Figure 2: Example of the impact of the synchronization in the routing decisions.

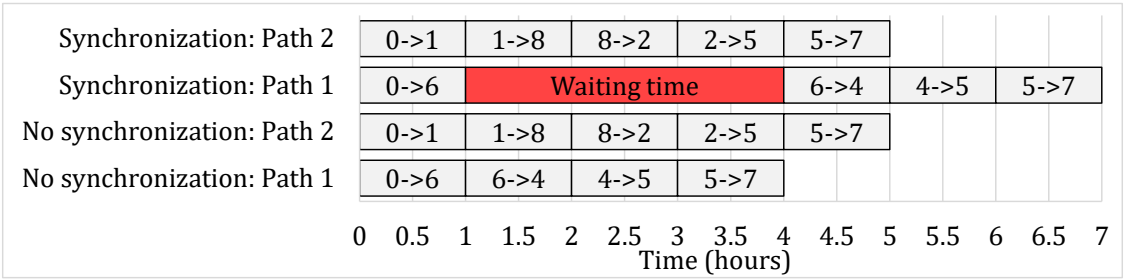

4 Mathematical formulations

In this section, we present three mixed integer programming formulations for the MCSRP and two families of valid inequalities to strengthen them. The first and second formulations differ in the way of modeling the scheduling decisions and the synchronization of the crews. The third formulation eliminates symmetry related to the routing decisions by dropping certain variables and imposing new types of constraints.

4.1 First MCSRP formulation (MCSRP1)

The first MCSRP formulation is based on the three-index vehicle flow formulation of the vehicle routing problem (VRP) (Irnich et al., 2014) to define the schedule of the crews, while the synchronization of the crews is controlled with a four-index variable. The mathematical notation is as follows.

Sets

$\mathcal{V}$	All nodes.
$\mathcal{V}^{\mathtt{r}} \subset \mathcal{V}$	Damaged nodes.
$\mathcal{V}_0^{\mathtt{r}} = \mathcal{V}^{\mathtt{r}} \cup \{0\}$	Damaged nodes including the source node 0 (depot).
$\mathcal{V}^{\mathtt{u}} \subset \mathcal{V}$	Undamaged nodes ($\mathcal{V}^{\mathtt{u}} = \mathcal{V} \setminus \mathcal{V}^{\mathtt{r}}$).
$\mathcal{V}^{\mathtt{d}} \subset \mathcal{V}$	Demand nodes.
E	Arcs.
$E_i \subseteq E$	Arcs incident to node $i \in \mathcal{V}$.
$\mathcal{R} = \{1, \cdots, \lvert\mathcal{V}^{\mathtt{r}}\rvert\}$	Positions at which an already repaired damaged node can be visited in a path between two damaged nodes.
$\mathcal{K}$	Available crews.
$\mathcal{K}_i \subseteq \mathcal{K}$	Crews able to repair the damaged node $i \in \mathcal{V}^{\mathtt{r}}$.

Parameters

d_i	Demand of node $i \in \mathcal{V}^{\mathtt{d}}$.
δ_{ki}	Repair time of crew $k \in \mathcal{K}_i$ at node $i \in \mathcal{V}^{\mathtt{r}}$.
τ_{ke}	Travel time of crew $k \in \mathcal{K}$ on arc $e \in E$.
ρ_{kij}	Shortest travel time of crew k between nodes $i \in \mathcal{V}$ and $j \in \mathcal{V}$ without using damaged nodes.
ℓ_e	Length of arc $e \in E$.
$l_i^{\mathtt{d}}$	Maximum distance allowed between node 0 and demand node $i \in \mathcal{V}^{\mathtt{d}}$.
M	Sufficiently large number.

Decision variables

W_i Binary variable that assumes the value of 1 if and only if node $i \in \mathcal{V}^{\mathtt{r}}$ is repaired.

X_{kij} Binary variable that assumes the value of 1 if and only if crew $k \in \mathcal{K}$ repairs node $j \in \mathcal{V}_0^{\mathtt{r}}$ immediately after node $i \in \mathcal{V}_0^{\mathtt{r}}$.

P_{eij} Binary variable that assumes the value of 1 if and only if arc $e \in E$ is used in the path from node $i \in \mathcal{V}_0^{\mathtt{r}}$ to node $j \in \mathcal{V}^{\mathtt{r}}$.

$N_{lij}^{\mathtt{u}}$ Binary variable that assumes the value of 1 if and only if node $l \in \mathcal{V}^{\mathtt{u}}$ is used in the path from node $i \in \mathcal{V}_0^{\mathtt{r}}$ to node $j \in \mathcal{V}^{\mathtt{r}}$.

$N_{lhij}^{\mathtt{r}}$ Binary variable that assumes the value of 1 if and only if node $l \in \mathcal{V}^{\mathtt{r}}$ is the hth damaged node visited in the path from node $i \in \mathcal{V}_0^{\mathtt{r}}$ to node $j \in \mathcal{V}^{\mathtt{r}}$.

Y_{ej} Binary variable that assumes the value of 1 if and only if arc $e \in E$ is used in the path from node 0 to node $j \in \mathcal{V}^{\mathtt{d}}$.

V_{lj} Binary variable that assumes the value of 1 if and only if node $l \in \mathcal{V}$ is used in the path from node 0 to node $j \in \mathcal{V}^{\mathtt{d}}$.

$T_{lhj}^{\mathtt{s}}$ Time at which the crew assigned to repair damaged node $j \in \mathcal{V}^{\mathtt{r}}$ visits the damaged node $l \in \mathcal{V}^{\mathtt{r}}$ in the position $h \in \mathcal{R}$ in the path to node $j \in \mathcal{V}^{\mathtt{r}}$ (arrival time).

$T_{lhj}^{\mathtt{w}}$ Waiting time of the crew assigned to repair damaged node $j \in \mathcal{V}^{\mathtt{r}}$ at the damaged node $l \in \mathcal{V}^{\mathtt{r}}$ visited in the position $h \in \mathcal{R}$ in the path to node $j \in \mathcal{V}^{\mathtt{r}}$.

$Z_i^{\mathtt{r}}$ Restoration time of damaged node $i \in \mathcal{V}_0^{\mathtt{r}}$.

$Z_i^{\mathtt{d}}$ Accessibility time of demand node $i \in \mathcal{V}^{\mathtt{d}}$.

The parameter ρ_{kij} is computed by solving multiple shortest path problems over a graph in which the damaged nodes and arcs incident to the damaged nodes have been removed. In some cases, the removal of the damaged nodes can result in multiple unconnected graph components in the graph. In these cases, there are no paths between some pair of nodes $i - j$ without using at least one damaged node, and ρ_{kij} is assumed to be a sufficiently large number.

The variables X_{kij} define the schedule of the crews, while their route is defined by variables P_{eij}, $N_{lij}^{\mathtt{u}}$ and $N_{lhij}^{\mathtt{r}}$, which determine the arcs and nodes to be visited in a crew path $i - j$. Variable $N_{lhij}^{\mathtt{r}}$ controls the position h of the damaged node l visited in such a path. The position is used to synchronize the arrival and departure of the crews at the damaged nodes. Since no synchronization is necessary for the undamaged nodes, the position at which a node $l \in \mathcal{V}^{\mathtt{u}}$ is visited by the crews is not relevant. Variables P_{eij}, $N_{lij}^{\mathtt{d}}$ and $N_{lhij}^{\mathtt{r}}$ are not defined for $j = 0$ since we assume that the crews return to the depot using any feasible path composed of either repaired damaged nodes and/or undamaged nodes. Finally, variables Y_{ej} and V_{lj} define the arcs and nodes, respectively, to be visited in relief path $0-j$. The MIP model is formulated as follows.

Objective function. The objective function (1) consists of minimizing the weighted sum of the accessibility time.

$$\min \sum_{i \in \mathcal{V}^{\mathtt{d}}} d_i \cdot Z_i^{\mathtt{d}}. \tag{1}$$

Accessibility time evaluation. The accessibility time is defined by constraints (2). A demand node i is accessible if there exists a relief path $0 - i$ using undamaged and/or repaired nodes.

Thus, the accessibility time $Z_i^{\mathtt{d}}$ associated with demand node $i \in \mathcal{V}^{\mathtt{d}}$ depends on the time $Z_j^{\mathtt{r}}$ when damaged nodes $j \in \mathcal{V}^{\mathtt{r}}$ in relief path $0-i$ are repaired.

$$Z_i^{\mathtt{d}} \geq Z_j^{\mathtt{r}} - M \cdot (1 - V_{ji}),\ \forall\ i \in \mathcal{V}^{\mathtt{d}},\ j \in \mathcal{V}^{\mathtt{r}}. \tag{2}$$

Restoration time constraints. Constraints (3) define the restoration time when no damaged nodes are visited in crew path $i-j$ or when there is no waiting time associated with the visited damaged nodes. In this case, for a given node j repaired by crew k, the restoration time $Z_j^{\mathtt{r}}$ is the sum of three components: the restoration time of the predecessor node i ($Z_i^{\mathtt{r}}$); the travel time in the path $i-j$ ($\sum_{e \in E} \tau_{ke} \cdot P_{eij}$); and the repair time of node j (δ_{kj}). These constraints also prevent subtours. Constraints (4) define the restoration time when there is waiting time associated with the damaged nodes visited in a given path $i-j$. In this case, for a given node j repaired by crew k, the restoration time $Z_j^{\mathtt{r}}$ is the sum of the next components: the time when the crew departs from the last damaged node l visited in the path ($T_{lhj}^{\mathtt{w}} + T_{lhj}^{\mathtt{s}}$); the shortest travel time from node l to node j without using damaged nodes ($\sum_{i \in \mathcal{V}_0^{\mathtt{r}}} \rho_{klj} \cdot N_{lhij}^{\mathtt{r}}$); and the repair time of node j (δ_{kj}). Constraints (4) are activated only for the last occupied position h, i.e., when there is no node visited in the position $h+1$ ($\sum_{i \in \mathcal{V}_0^{\mathtt{r}}} \sum_{l \in \mathcal{V}^r} N_{l(h+1)ij}^{\mathtt{r}} = 0$).

$$Z_j^{\mathtt{r}} \geq Z_i^{\mathtt{r}} + \sum_{e \in E} \tau_{ke} \cdot P_{eij} + \delta_{kj} - M \cdot (1 - X_{kij}),\ \forall\ i \in \mathcal{V}_0^{\mathtt{r}},\ j \in \mathcal{V}^{\mathtt{r}},\ k \in \mathcal{K}, \tag{3}$$

$$Z_j^{\mathtt{r}} \geq \sum_{l \in \mathcal{V}^{\mathtt{r}}} (T_{lhj}^{\mathtt{w}} + T_{lhj}^{\mathtt{s}} + \sum_{i \in \mathcal{V}_0^{\mathtt{r}}} \rho_{klj} \cdot N_{lhij}^{\mathtt{r}}) + \delta_{kj} - M \cdot (1 - \sum_{i \in \mathcal{V}_0^{\mathtt{r}}} X_{kij} + \sum_{i \in \mathcal{V}_0^{\mathtt{r}}} \sum_{l \in \mathcal{V}^{\mathtt{r}}} N_{l(h+1)ij}^{\mathtt{r}}),$$
$$\forall\ j \in \mathcal{V}^{\mathtt{r}},\ h \in \mathcal{R} \setminus \{|\mathcal{R}|\},\ k \in \mathcal{K}. \tag{4}$$

Relief path constraints. For a given relief path $0-i$, constraints (5) force the use of an arc incident to node 0, while constraints (6) force the use of an arc incident to node i. Furthermore, for each node l in the middle of this path ($V_{li} = 1$), there must be one arc leaving and one arc arriving at node l, as imposed by constraints (7). Constraints (8) prohibit the use of relief paths whose distance between the depot and demand nodes is greater than the maximum distance allowed. Note that constraints (8) can be relaxed by considering sufficiently large numbers for the maximum distance $l_i^{\mathtt{d}}$.

$$\sum_{e \in E_0} Y_{ei} = 1,\ \forall\ i \in \mathcal{V}^{\mathtt{d}}, \tag{5}$$

$$\sum_{e \in E_i} Y_{ei} = 1,\ \forall\ i \in \mathcal{V}^{\mathtt{d}}, \tag{6}$$

$$\sum_{e \in E_l} Y_{ei} = 2V_{li},\ \forall\ j \in \mathcal{V}^{\mathtt{d}},\ l \in \mathcal{V} \setminus \{0,\ i\}, \tag{7}$$

$$\sum_{e \in E} Y_{ei} \cdot \ell_e \leq l_i^{\mathtt{d}},\ \forall\ i \in \mathcal{V}^{\mathtt{d}}. \tag{8}$$

Crew routing constraints. If there is a crew path $i-j$ ($\sum_{k \in \mathcal{K}} X_{kij} = 1$), constraints (9) force the use of an arc incident to node i in this path, while constraints (10) force the use of an arc incident to node j. Given a node l in crew path $i-j$, constraints (11) and (12) ensure that

path $i-j$ contains one arc leaving node l and one arc arriving at node l. Constraints (11) are associated with undamaged nodes $l \in \mathcal{V}^{\mathtt{u}}$, while constraints (12) are associated with damaged nodes $l \in \mathcal{V}^{\mathtt{r}}$.

$$\sum_{e \in E_i} P_{eij} = \sum_{k \in \mathcal{K}} X_{kij}, \forall\ i \in \mathcal{V}_0^{\mathtt{r}},\ j \in \mathcal{V}^{\mathtt{r}}, \tag{9}$$

$$\sum_{e \in E_j} P_{eij} = \sum_{k \in \mathcal{K}} X_{kij}, \forall\ i \in \mathcal{V}_0^{\mathtt{r}},\ j \in \mathcal{V}^{\mathtt{r}}, \tag{10}$$

$$\sum_{e \in E_l} P_{eij} = 2N_{lij}^{\mathtt{u}}, \forall\ i \in \mathcal{V}_0^{\mathtt{r}},\ j \in \mathcal{V}^{\mathtt{r}},\ l \in \mathcal{V}^{\mathtt{u}} : l \neq i, \tag{11}$$

$$\sum_{e \in E_l} P_{eij} = 2 \sum_{h \in \mathcal{R}} N_{lhij}^{\mathtt{r}}, \forall\ i \in \mathcal{V}_0^{\mathtt{r}},\ j \in \mathcal{V}^{\mathtt{r}},\ l \in \mathcal{V}^{\mathtt{r}} \setminus \{i,\ j\}. \tag{12}$$

Crew scheduling constraints. If node j is repaired ($W_j = 1$), constraints (13) state that there will be exactly one crew $k \in \mathcal{K}_j$ designated to repair this node. Constraints (14) represent the flow conservation. Constraints (15) establish that each crew k must perform at most one schedule.

$$\sum_{k \in \mathcal{K}_j} \sum_{\substack{i \in \mathcal{V}_0^{\mathtt{r}}: \\ i \neq l}} X_{kij} = W_j, \forall\, j \in \mathcal{V}^{\mathtt{r}}, \tag{13}$$

$$\sum_{\substack{i \in \mathcal{V}_0^{\mathtt{r}}: \\ i \neq l}} X_{kil} - \sum_{\substack{j \in \mathcal{V}_0^{\mathtt{r}}: \\ j \neq l}} X_{klj} = 0, \forall\ l \in \mathcal{V}_0^{\mathtt{r}},\ k \in \mathcal{K}, \tag{14}$$

$$\sum_{j \in \mathcal{V}^{\mathtt{r}}} X_{k0j} \leq 1, \forall\, k \in \mathcal{K}. \tag{15}$$

Assignment constraints. Constraints (16) and (17) state that node $l \in \mathcal{V}^{\mathtt{r}}$ must be repaired if it is used in either a relief path ($\sum_{i \in \mathcal{V}^{\mathtt{d}}} V_{li} > 1$) or a crew path ($\sum_{h \in \mathcal{R}} \sum_{i \in \mathcal{V}_0^{\mathtt{r}}} \sum_{j \in \mathcal{V}^{\mathtt{r}}} N_{lhij}^{\mathtt{r}} > 1$).

$$|\mathcal{V}^{\mathtt{d}}| \cdot W_l \geq \sum_{i \in \mathcal{V}^{\mathtt{d}}} V_{li}, \forall\, l \in \mathcal{V}^{\mathtt{r}}, \tag{16}$$

$$|\mathcal{V}^{\mathtt{r}}| \cdot W_l \geq \sum_{h \in \mathcal{R}} \sum_{i \in \mathcal{V}_0^{\mathtt{r}}} \sum_{j \in \mathcal{V}^{\mathtt{r}}} N_{lhij}^{\mathtt{r}}, \forall\, l \in \mathcal{V}^{\mathtt{r}}. \tag{17}$$

Synchronization constraints. Constraints (18)-(23) synchronize the arrival of crew k in damaged node l visited in crew path $i-j$. Here, i and j are damaged nodes repaired by crew k, while l is a damaged node used in path $i-j$. Thus, when crew k arrives at this node l, it either waits for node l to be repaired by another crew if this node is still damaged, or it can cross without waiting if l has already been repaired. Constraints (18) guarantee that a damaged node l cannot be visited more than once in the path to node j. Since all the travel times on the arcs are nonnegative values, the optimal crew path $i-j$ does not need to consider a node l more than once. Constraints (19) establish that a given crew cannot visit different damaged nodes simultaneously, i.e., a position h can be occupied for at most one damaged node l in the path to node j. Constraints (20) ensure that damaged nodes in path $i-j$ must be visited in

consecutive positions. Then, a damaged node cannot be visited in a position h if no damaged node was already visited in position $h-1$. Constraints (21) evaluate the arrival time of crew k at the first damaged node l visited in path $i-j$. Similarly, constraints (22) define the arrival time of crew k at the damaged node l visited in position $h>1$ based on the departure time of node v visited in position $h-1$. Finally, constraints (23) compute the waiting time of the crew in damaged node l visited in position h. The waiting time is calculated as the difference between the restoration time of the damaged node l and the arrival time of crew k at damaged node l.

$$\sum_{h\in\mathcal{R}}\sum_{i\in\mathcal{V}_0^{\mathtt{r}}} N^{\mathtt{r}}_{lhij} \leq 1,\ \forall\ l\in\mathcal{V}^{\mathtt{r}},\ j\in\mathcal{V}^{\mathtt{r}}, \tag{18}$$

$$\sum_{l\in\mathcal{V}^{\mathtt{r}}}\sum_{i\in\mathcal{V}_0^{\mathtt{r}}} N^{\mathtt{r}}_{lhij} \leq 1,\ \forall\ h\in\mathcal{R},\ j\in\mathcal{V}^{\mathtt{r}}, \tag{19}$$

$$\sum_{l\in\mathcal{V}^{\mathtt{r}}} N^{\mathtt{r}}_{lhij} \leq \sum_{l\in\mathcal{V}^{\mathtt{r}}} N^{\mathtt{r}}_{l(h-1)ij},\ \forall\ i\in\mathcal{V}_0^{\mathtt{r}},\ j\in\mathcal{V}^{\mathtt{r}},\ h\in\mathcal{R}\setminus\{1\}, \tag{20}$$

$$T^{\mathtt{s}}_{l1j} \geq Z^{\mathtt{r}}_i + \sum_{k\in\mathcal{K}} \rho_{kil}\cdot X_{kij} - M\cdot(1-N^{\mathtt{r}}_{l1ij}),\ \forall\ i\in\mathcal{V}_0^{\mathtt{r}},\ j\in\mathcal{V}^{\mathtt{r}},\ l\in\mathcal{V}^{\mathtt{r}}, \tag{21}$$

$$T^{\mathtt{s}}_{lhj} \geq \sum_{v\in\mathcal{V}^{\mathtt{r}}}(T^{\mathtt{w}}_{v(h-1)j} + T^{\mathtt{s}}_{v(h-1)j} + \sum_{i\in\mathcal{V}_0^{\mathtt{r}}} N^{\mathtt{r}}_{v(h-1)ij}\cdot\rho_{kvl}) - M\cdot(2-\sum_{i\in\mathcal{V}_0^{\mathtt{r}}}(N^{\mathtt{r}}_{lhij}+X_{kij})),$$
$$\forall\ k\in\mathcal{K}, l\in\mathcal{V}^{\mathtt{r}}, j\in\mathcal{V}^{\mathtt{r}},\ h\in\mathcal{R}\setminus\{1\}, \tag{22}$$

$$T^{\mathtt{w}}_{lhj} \geq Z^{\mathtt{r}}_l - T^{\mathtt{s}}_{lhj} - M\cdot(1-\sum_{i\in\mathcal{V}_0^{\mathtt{r}}} N^{\mathtt{r}}_{lhij}),\ \forall\ l\in\mathcal{V}^{\mathtt{r}},\ j\in\mathcal{V}^{\mathtt{r}},\ h\in\mathcal{R}. \tag{23}$$

Domain of the decision variables. Constraints (24)-(31) impose the domain of the decision variables. It is worth mentioning that variables P_{eij} and Y_{ej} do not need to be defined as binary variables in the computational implementation because they naturally assume binary values if variables $N^{\mathtt{u}}_{lij}$, $N^{\mathtt{r}}_{lhij}$ and V_{kj} are binaries.

$$X_{kij}, W_j \in \{0,1\},\ \forall\ i\in\mathcal{V}_0^{\mathtt{r}},\ j\in\mathcal{V}_0^{\mathtt{r}},\ k\in\mathcal{K}, \tag{24}$$

$$N^{\mathtt{r}}_{lhij} \in \{0,1\},\ \forall\ i\in\mathcal{V}_0^{\mathtt{r}},\ j\in\mathcal{V}^{\mathtt{r}},\ l\in\mathcal{V}^{\mathtt{r}},\ h\in\mathcal{R}, \tag{25}$$

$$N^{\mathtt{u}}_{lij} \in \{0,1\},\ \forall\ i\in\mathcal{V}_0^{\mathtt{r}},\ j\in\mathcal{V}^{\mathtt{r}},\ l\in\mathcal{V}^{\mathtt{u}}, \tag{26}$$

$$P_{eij} \geq 0,\ \forall\ i\in\mathcal{V}_0^{\mathtt{r}},\ j\in\mathcal{V}^{\mathtt{r}},\ e\in E, \tag{27}$$

$$V_{li} \in \{0,1\},\ \forall\ i\in\mathcal{V}^{\mathtt{d}},\ l\in\mathcal{V}, \tag{28}$$

$$Y_{el} \geq 0,\ \forall\ l\in\mathcal{V}^{\mathtt{d}},\ e\in E, \tag{29}$$

$$T^{\mathtt{s}}_{lhj}, T^{\mathtt{w}}_{lhj} \geq 0,\ \forall\ l\in\mathcal{V}^{\mathtt{r}}, j\in\mathcal{V}^{\mathtt{r}},\ h\in\mathcal{R}, \tag{30}$$

$$Z^{\mathtt{r}}_i, Z^{\mathtt{d}}_j \geq 0,\ \forall\ i\in\mathcal{V}_0^{\mathtt{r}},\ j\in\mathcal{V}^{\mathtt{d}}. \tag{31}$$

4.2 Second MCSRP formulation (MCSRP2)

The second formulation for the MCSRP is based on the two-index vehicle flow formulation of the VRP to define the crew scheduling, while the synchronization of the crews is controlled with a new three-index variable. For this formulation, consider the following notation:

Decision variables

W'_{ik} Binary variable that assumes the value of 1 if and only if node $i \in \mathcal{V}^{\mathrm{r}}$ is repaired by crew k.

X'_{ij} Binary variable that assumes the value of 1 if and only if node $j \in \mathcal{V}^{\mathrm{r}}_0$ is repaired immediately after node $i \in \mathcal{V}^{\mathrm{r}}_0$.

N_{lij} Binary variable that assumes the value of 1 if and only if node $l \in \mathcal{V}$ is visited in the path from node $i \in \mathcal{V}^{\mathrm{r}}_0$ to node $j \in \mathcal{V}^{\mathrm{r}}$.

R_{lhj} Binary variable that assumes the value of 1 if and only if node $l \in \mathcal{V}^{\mathrm{r}}$ is the hth damaged node visited in the path to node $j \in \mathcal{V}^{\mathrm{r}}$.

The two-index variable X'_{ij} defines the restoration order of the damaged nodes, independent of the crew that performs this activity. The assignment of the crews to the damaged nodes is achieved with variable W'_{ik}. Furthermore, the position of the damaged nodes in the crew paths is controlled with the new variable R_{lhj}. The objective function (1), the accessibility time evaluation (2), and the relief paths constraints (5)-(8) are the same as in MCSRP1. The other group of constraints is modified as follows.

Restoration time and crew routing and scheduling constraints. In constraints (32)-(38), we use variables X'_{ij} and/or W'_{kj} instead of X_{kij} and/or W_j. Additionally, in constraints (33), variable R_{lhj} is used instead of N^{r}_{lhij}, and in constraints (39), variable N_{lij} is used instead of N^{r}_{lhij}. Constraints (39) control the arcs incident to any node $l \in \mathcal{V}$ in a given path $i-j$ instead of constraints (11) and (12) that are associated with undamaged nodes $l \in \mathcal{V}^{\mathrm{u}}$ and damaged nodes $l \in \mathcal{V}^{\mathrm{r}}$ separately. Furthermore, unlike MCSRP1, the flow conservation constraints (34) are not defined for each crew.

$$Z^{\mathrm{r}}_j \geq Z^{\mathrm{r}}_i + \sum_{e \in E} \tau_{ke} \cdot P_{eij} + \delta_{kj} - M \cdot (2 - X'_{ij} - W'_{kj}), \; \forall \; i \in \mathcal{V}^{\mathrm{r}}, \; j \in \mathcal{V}^{\mathrm{r}}, \; k \in \mathcal{K}, \tag{32}$$

$$Z^{\mathrm{r}}_j \geq \sum_{l \in \mathcal{V}^{\mathrm{r}}} (T^{\mathrm{w}}_{lhj} + T^{\mathrm{s}}_{lhj} + \rho_{klj} \cdot R_{lhj}) + \delta_{kj} - M \cdot (1 - W'_{kj} + \sum_{l \in \mathcal{V}^{\mathrm{r}}} R_{(h+1)lj}),$$

$$\forall \; j \in \mathcal{V}^{\mathrm{r}}, \; h \in \mathcal{R} \setminus \{|\mathcal{R}|\}, \; k \in \mathcal{K}, \tag{33}$$

$$\sum_{\substack{i \in \mathcal{V}^{\mathrm{r}}_0: \\ i \neq j}} X'_{ij} = \sum_{k \in \mathcal{K}} W'_{kj}, \; \forall \, j \in \mathcal{V}^{\mathrm{r}}, \tag{34}$$

$$\sum_{\substack{i \in \mathcal{V}^{\mathrm{r}}_0: \\ i \neq l}} X'_{il} - \sum_{\substack{j \in \mathcal{V}^{\mathrm{r}}_0: \\ j \neq l}} X'_{lj} = 0, \; \forall \; l \in \mathcal{V}^{\mathrm{r}}_0, \tag{35}$$

$$\sum_{j \in \mathcal{V}^{\mathrm{r}}} X'_{0j} \leq |\mathcal{K}|, \tag{36}$$

$$\sum_{e \in E_i} P_{eij} = X'_{ij}, \; \forall \; i \in \mathcal{V}^{\mathrm{r}}_0, \; j \in \mathcal{V}^{\mathrm{r}}, \tag{37}$$

$$\sum_{e \in E_j} P_{eij} = X'_{ij}, \; \forall \; i \in \mathcal{V}^{\mathrm{r}}_0, \; j \in \mathcal{V}^{\mathrm{r}}, \tag{38}$$

$$\sum_{e \in E_l} P_{eij} = 2N_{lij}, \; \forall \; i \in \mathcal{V}^{\mathrm{r}}_0, \; j \in \mathcal{V}^{\mathrm{r}}, \; l \in \mathcal{V} \setminus \{i, \; j\}. \tag{39}$$

Assignment constraints. Constraints (40) and (41) define which nodes must be repaired. Additionally, constraints (42) are introduced to guarantee that if nodes i and j are considered in the same schedule ($X'_{ij} = 1$), both are repaired by the same crew. Constraints (43) force the consideration of different crews for different schedules. If $X_{0i} = 1$ and $X_{0j} = 1$, i and j are the first nodes of two different schedules. Thus, if crew k repairs node i ($W'_{ki} = 1$), a different crew k' must repair node j, i.e., $\sum_{\substack{k' \in \mathcal{K}: \\ k' \neq k}} W_{k'j} \geq 1$.

$$|\mathcal{V}^{\mathrm{r}}| \cdot \sum_{k \in \mathcal{K}_l} W'_{kl} \geq \sum_{i \in \mathcal{V}_0^{\mathrm{r}}} \sum_{j \in \mathcal{V}^{\mathrm{r}}} N_{lij}, \forall\, l \in \mathcal{V}^{\mathrm{r}}, \tag{40}$$

$$|\mathcal{V}^{\mathrm{d}}| \cdot \sum_{k \in \mathcal{K}_l} W'_{kl} \geq \sum_{i \in \mathcal{V}^{\mathrm{d}}} V_{li}, \forall\, l \in \mathcal{V}^{\mathrm{r}}, \tag{41}$$

$$W'_{kj} \geq W'_{ki} + X'_{ij} - 1, \forall\, i \in \mathcal{V}^{\mathrm{r}},\ j \in \mathcal{V}^{\mathrm{r}},\ k \in \mathcal{K}, \tag{42}$$

$$\sum_{\substack{k' \in \mathcal{K}: \\ k' \neq k}} W_{k'j} \geq W_{ki} + X_{0i} + X_{0j} - 2, \forall\, i \in \mathcal{V}^{\mathrm{r}},\ j \in \mathcal{V}^{\mathrm{r}} : i \neq j,\ k \in \mathcal{K}. \tag{43}$$

Synchronization constraints. The new set of constraints (44) is introduced to enforce the allocation of damaged nodes l considered in path $i - j$ ($N_{lij} = 1$) to some position h defined by variable R_{lhj}. Constraints (45)-(47) define the position of a damaged node l in the path to node j. Constraints (48)-(50) define the arrival and waiting time of the crews at the damaged node l visited in the path from node i to node j.

$$\sum_{i \in \mathcal{V}_0^{\mathrm{r}}} N_{lij} = \sum_{h \in \mathcal{R}} R_{lhj}, \forall\, l \in \mathcal{V}^{\mathrm{r}},\ j \in \mathcal{V}^{\mathrm{r}}, \tag{44}$$

$$\sum_{h \in \mathcal{R}} R_{lhj} \leq 1, \forall\, j \in \mathcal{V}^{\mathrm{r}},\ l \in \mathcal{V}^{\mathrm{r}}, \tag{45}$$

$$\sum_{l \in \mathcal{V}^{\mathrm{r}}} R_{lhj} \leq 1, \forall\, j \in \mathcal{V}^{\mathrm{r}},\ h \in \mathcal{R}, \tag{46}$$

$$\sum_{l \in \mathcal{V}^{\mathrm{r}}} R_{lhj} \leq \sum_{l \in \mathcal{V}^{\mathrm{r}}} R_{(h-1)lj}, \forall\, j \in \mathcal{V}^{\mathrm{r}},\ h \in \mathcal{R} \setminus \{1\}, \tag{47}$$

$$T^{\mathrm{s}}_{l1j} \geq Z^{\mathrm{r}}_i + \sum_{k \in \mathcal{K}} W'_{kj} \cdot \rho_{kil} - (2 - X'_{ij} - R_{l1j}) \cdot M, \forall\, i \in \mathcal{V}_0^{\mathrm{r}},\ j \in \mathcal{V}^{\mathrm{r}},\ l \in \mathcal{V}^{\mathrm{r}}, \tag{48}$$

$$T^{\mathrm{s}}_{lhj} \geq \sum_{p \in \mathcal{V}^{\mathrm{r}}} (T^{\mathrm{w}}_{(h-1)pj} + T^{\mathrm{s}}_{(h-1)pj} + R_{(h-1)pj} \cdot \rho_{kpl}) - (2 - R_{lhj} - W'_{kj}) \cdot M,$$
$$\forall\, k \in \mathcal{K}, l \in \mathcal{V}^{\mathrm{r}}, j \in \mathcal{V}^{\mathrm{r}},\ h \in \mathcal{R} \setminus \{1\}, \tag{49}$$

$$T^{\mathrm{w}}_{lhj} \geq Z^{\mathrm{r}}_l - T^{\mathrm{s}}_{lhj} - M \cdot (1 - R_{lhj}), \forall\, l \in \mathcal{V}^{\mathrm{r}},\ j \in \mathcal{V}^{\mathrm{r}},\ h \in \mathcal{R}. \tag{50}$$

Domain of the decision variables. Constraints (51) and (53) impose the domain of the decision variables.

$$X'_{ij}, W'_{kj} \in \{0, 1\}, \forall\, i \in \mathcal{V}_0^{\mathrm{r}},\ j \in \mathcal{V}_0^{\mathrm{r}},\ k \in \mathcal{K}, \tag{51}$$

$$R_{hij} \in \{0, 1\}, \forall\, i \in \mathcal{V}^{\mathrm{r}},\ j \in \mathcal{V}^{\mathrm{r}},\ h \in \mathcal{R}, \tag{52}$$

$$N_{lij} \in \{0, 1\}, \forall\, i \in \mathcal{V}_0^{\mathrm{r}},\ j \in \mathcal{V}^{\mathrm{r}},\ l \in \mathcal{V}. \tag{53}$$

4.3 Third MCSRP formulation (MCSRP3)

The third formulation is a modified version of MCSRP2 with the elimination of some variables related to the routing decisions. Furthermore, some additional constraints are introduced to prohibit the restoration of the damaged nodes that do not affect the accessibility of the demand nodes. For instance, consider the schedule (0, 1, 2, 0) for one crew and assume that damaged node 2 is not considered either in the relief paths or in the crew paths. Then, the restoration time of node 2 does not affect the accessibility of the demand nodes. In this case, several solutions considering different crew paths from node 1 to node 2 have the same cost as the solution considering the schedule (0, 1, 0). We say that such solutions are symmetric and can be eliminated by prohibiting the restoration of unnecessary damaged nodes. For the MCSRP3, consider the additional notation as follows.

Decision variables

P'_{eij} Binary variable that assumes the value of 1 if and only if arc $e \in E$ is used either in the path from node $i \in \mathcal{V}^{\mathrm{r}}_0$ to node $j \in \mathcal{V}^{\mathrm{r}}$ or from node $j \in \mathcal{V}^{\mathrm{r}}$ to node $i \in \mathcal{V}^{\mathrm{r}}$ with $i < j$.

N'_{lij} Binary variable that assumes the value of 1 if and only if node $l \in \mathcal{V}^{\mathrm{r}}$ is used either in the path from node $i \in \mathcal{V}^{\mathrm{r}}_0$ to node $j \in \mathcal{V}^{\mathrm{r}}$ or from node $j \in \mathcal{V}^{\mathrm{r}}$ to node $i \in \mathcal{V}^{\mathrm{r}}$ with $i < j$.

Variables P'_{eij} and N'_{lij} are defined only for path $i - j$, where $i < j$. The objective function (1), the accessibility time evaluation (2), the relief paths constraints (5)-(8), and the scheduling constraints (34)-(36) are the same as in MCSRP2. The other constraints are posed as follows.

Restoration time constraints. Constraints (54) and (55) define the restoration time at the damaged nodes when $i < j$ and $i > j$, respectively. Constraints (33) are also included in MCSRP3.

$$Z^{\mathrm{r}}_j \geq Z^{\mathrm{r}}_i + \sum_{e \in E} \tau_{ke} \cdot P'_{eij} + \delta_{kj} - (2 - X'_{ij} - W'_{kj}) \cdot M, \forall\, k \in \mathcal{K},\, i \in \mathcal{V}^{\mathrm{r}}_0,\; j \in \mathcal{V}^{\mathrm{r}} : i < j, \tag{54}$$

$$Z^{\mathrm{r}}_j \geq Z^{\mathrm{r}}_i + \sum_{e \in E} \tau_{ke} \cdot P'_{eji} + \delta_{kj} - (2 - X'_{ij} - W'_{kj}) \cdot M, \forall\, k \in \mathcal{K},\, i \in \mathcal{V}^{\mathrm{r}},\; j \in \mathcal{V}^{\mathrm{r}} : i > j. \tag{55}$$

Crew routing constraints. Constraints (56)-(60) define the paths of the crews for $i < j$ only.

$$\sum_{e \in E_0} P'_{e0j} = X'_{0j}, \forall\, j \in \mathcal{V}^{\mathrm{r}}, \tag{56}$$

$$\sum_{e \in E_j} P'_{e0j} = X'_{0j}, \forall\, j \in \mathcal{V}^{\mathrm{r}}, \tag{57}$$

$$\sum_{e \in E_i} P'_{eij} = X'_{ij} + X'_{ji}, \forall\, i \in \mathcal{V}^{\mathrm{r}},\; j \in \mathcal{V}^{\mathrm{r}} : i < j, \tag{58}$$

$$\sum_{e \in E_j} P'_{eij} = X'_{ij} + X'_{ji}, \forall\, i \in \mathcal{V}^{\mathrm{r}},\; j \in \mathcal{V}^{\mathrm{r}} : i < j, \tag{59}$$

$$\sum_{e \in E_l} P'_{eij} = 2N'_{lij}, \forall\, i \in \mathcal{V}^{\mathrm{r}}_0,\; j \in \mathcal{V}^{\mathrm{r}},\; l \in \mathcal{V} \setminus \{i,\; j\} : i < j. \tag{60}$$

Assignment constraints. Constraints (61) replace constraints (40) to force the restoration of nodes used in crew paths $i - j$ with $i < j$. Constraints (62) are introduced to prohibit

the restoration of some unnecessary damaged nodes. Thus, the last damaged node l repaired by a crew ($X'_{l0} = 1$) must be used either in a relief path ($\sum_{i \in \mathcal{V}^{\mathrm{d}}} V_{li} > 1$) or in a crew path ($\sum_{i \in \mathcal{V}_0^{\mathrm{r}}} \sum_{\substack{j \in \mathcal{V}^{\mathrm{r}}: \\ i<j}} N'_{lij} > 1$). Constraints (41)-(43) are also included in MCSRP3.

$$|\mathcal{V}^{\mathrm{r}}| \cdot \sum_{k \in \mathcal{K}_l} W'_{kl} \geq \sum_{i \in \mathcal{V}_0^{\mathrm{r}}} \sum_{\substack{j \in \mathcal{V}^{\mathrm{r}}: \\ i<j}} N'_{lij}, \forall\, l \in \mathcal{V}^{\mathrm{r}}, \tag{61}$$

$$\sum_{k \in \mathcal{K}_l} W'_{kl} \leq \sum_{i \in \mathcal{V}^{\mathrm{d}}} V_{li} + \sum_{i \in \mathcal{V}_0^{\mathrm{r}}} \sum_{\substack{j \in \mathcal{V}^{\mathrm{r}}: \\ i<j}} N'_{lij} - X'_{l0} + 1, \forall\, l \in \mathcal{V}^{\mathrm{r}}. \tag{62}$$

Synchronization constraints. Constraints (63)-(65) enforce the allocation of damaged nodes l considered in crew path $i-j$ to some position h defined by variable R_{lhj}. Constraints (45)-(50) are also included in MCSRP3.

$$\sum_{h \in \mathcal{R}} R_{lhj} \geq N'_{lij} + X'_{ij} - 1, \forall\, i \in \mathcal{V}^{\mathrm{r}},\ l \in \mathcal{V}^{\mathrm{r}},\ j \in \mathcal{V}^{\mathrm{r}} : i < j, \tag{63}$$

$$\sum_{h \in \mathcal{R}} R_{lhi} \geq N'_{lij} + X'_{ji} - 1, \forall\, i \in \mathcal{V}^{\mathrm{r}},\ l \in \mathcal{V}^{\mathrm{r}},\ j \in \mathcal{V}^{\mathrm{r}} : i < j, \tag{64}$$

$$\sum_{h \in \mathcal{R}} \sum_{j \in \mathcal{V}^{\mathrm{r}}} R_{lhj} = \sum_{i \in \mathcal{V}_0^{\mathrm{r}}} \sum_{j \in \mathcal{V}^{\mathrm{r}}: i<j} N'_{lij}, \forall\, l \in \mathcal{V}^{\mathrm{r}}. \tag{65}$$

Domain of the decision variables. Finally, constraints (66) and (67) impose the domain of the decision variables introduced in MCSRP3.

$$N'_{lij} \in \{0, 1\}, \forall\, l \in \mathcal{V},\ i \in \mathcal{V}_0^{\mathrm{r}},\ j \in \mathcal{V}^{\mathrm{r}} : i < j, \tag{66}$$

$$P'_{eij} \geq 0, \forall\, e \in E, i \in \mathcal{V}_0^{\mathrm{r}},\ j \in \mathcal{V}^{\mathrm{r}} : i < j. \tag{67}$$

Table 2 summarizes the variables and constraints considered in the three MIP models and shows examples of the number of binary variables and constraints in two arbitrary instances of different sizes.

Note that the numbers of binary variables and constraints are strongly influenced by the number of damaged nodes $|\mathcal{V}^{\mathrm{r}}|$. Thus, small changes in the number of damaged nodes can have a significant impact on the size of the problem, and thus, on the difficulty of solving it. The number of demand nodes $|\mathcal{V}^{\mathrm{d}}|$ and crews $|\mathcal{K}|$ seem to have a smaller impact on the number of variables and constraints when compared with $|\mathcal{V}^{\mathrm{r}}|$. As can be observed in Table 2, the main shortcoming of MCSRP1 relies on the high number of binary variables, which is greatly influenced by the three-index variable X_{kij} and by the four-index variable N^{r}_{lhij}. In an effort to reduce the number of binary variables, we eliminate one index from these variables to come out with model MCSRP2. Furthermore, in model MCSRP2, we observe that variables N_{lij} and P_{eij} do not need to be defined for all the pairs of damaged nodes $i-j$. Thus, in model MCSRP3, we define these variables only for pair of damaged nodes $i-j$ such that $i < j$. In addition, we eliminate some symmetric solutions by prohibiting the restoration of unnecessary damaged nodes in model MCSRP3. In general, the number of variables considered in the models is reduced from

Table 2: Variables and constraints of the proposed MIP formulations.

	MCSRP1	MCSRP2	MCSRP3
Binary variables	$W_i, X_{kij}, N^{\mathtt{u}}_{lij}, N^{\mathtt{r}}_{lhij}, V_{lj}$	$W'_{ik}, X'_{ij}, N_{lij}, R_{lhj}, V_{lj}$	$W'_{ik}, X'_{ij}, N'_{lij}, R_{lhj}, V_{lj}$
Continuous variables	$P_{eij}, Y_{ej}, T^{\mathtt{s}}_{lhj}, T^{\mathtt{w}}_{lhj}, Z^{\mathtt{r}}_i, Z^{\mathtt{d}}_i$	$P_{eij}, Y_{ej}, T^{\mathtt{s}}_{lhj}, T^{\mathtt{w}}_{lhj}, Z^{\mathtt{r}}_i, Z^{\mathtt{d}}_i$	$P'_{eij}, Y_{ej}, T^{\mathtt{s}}_{lhj}, T^{\mathtt{w}}_{lhj}, Z^{\mathtt{r}}_i, Z^{\mathtt{d}}_i$
Objective function	(1)	(1)	(1)
Constraints	(2)-(31)	(2), (5)-(8), (27)-(53)	(2), (5)-(8), (28)-(31), (33)-(36), (41)-(43), (45)-(52), (54)-(67)
# of binary variables[1]	$\lvert\mathcal{V}^{\mathtt{r}}\rvert + \lvert\mathcal{V}^{\mathtt{r}}\rvert\lvert\mathcal{V}^{\mathtt{d}}\rvert + \lvert\mathcal{K}\rvert\lvert\mathcal{V}^{\mathtt{r}}\rvert^2 + \lvert\mathcal{V}^{\mathtt{u}}\rvert\lvert\mathcal{V}^{\mathtt{r}}\rvert^2 + \lvert\mathcal{R}\rvert\lvert\mathcal{V}^{\mathtt{r}}\rvert^3$	$\lvert\mathcal{V}^{\mathtt{r}}\rvert\lvert\mathcal{K}\rvert + \lvert\mathcal{V}^{\mathtt{r}}\rvert\lvert\mathcal{V}^{\mathtt{d}}\rvert + \lvert\mathcal{V}^{\mathtt{r}}\rvert^2 + \lvert\mathcal{V}\rvert\lvert\mathcal{V}^{\mathtt{r}}\rvert^2 + \lvert\mathcal{R}\rvert\lvert\mathcal{V}^{\mathtt{r}}\rvert^2$	$\lvert\mathcal{V}^{\mathtt{r}}\rvert\lvert\mathcal{K}\rvert + \lvert\mathcal{V}^{\mathtt{r}}\rvert\lvert\mathcal{V}^{\mathtt{d}}\rvert + \lvert\mathcal{V}^{\mathtt{r}}\rvert^2 + (\lvert\mathcal{V}\rvert/2)(\lvert\mathcal{V}^{\mathtt{r}}\rvert^2 - \lvert\mathcal{V}^{\mathtt{r}}\rvert) + \lvert\mathcal{R}\rvert\lvert\mathcal{V}^{\mathtt{r}}\rvert^2$
# of continuous variables[1]	$\lvert\mathcal{V}^{\mathtt{d}}\rvert + \lvert\mathcal{V}^{\mathtt{r}}\rvert + \lvert E\rvert\lvert\mathcal{V}^{\mathtt{d}}\rvert + \lvert E\rvert\lvert\mathcal{V}^{\mathtt{r}}\rvert^2 + 2\lvert\mathcal{R}\rvert\lvert\mathcal{V}^{\mathtt{r}}\rvert^2$	$\lvert\mathcal{V}^{\mathtt{d}}\rvert + \lvert\mathcal{V}^{\mathtt{r}}\rvert + \lvert E\rvert\lvert\mathcal{V}^{\mathtt{d}}\rvert + \lvert E\rvert\lvert\mathcal{V}^{\mathtt{r}}\rvert^2 + 2\lvert\mathcal{R}\rvert\lvert\mathcal{V}^{\mathtt{r}}\rvert^2$	$\lvert\mathcal{V}^{\mathtt{r}}\rvert + \lvert\mathcal{V}^{\mathtt{d}}\rvert + \lvert E\rvert\lvert\mathcal{V}^{\mathtt{d}}\rvert + (\lvert E\rvert/2)(\lvert\mathcal{V}^{\mathtt{r}}\rvert^2 - \lvert\mathcal{V}^{\mathtt{r}}\rvert) + 2\lvert\mathcal{R}\rvert\lvert\mathcal{V}^{\mathtt{r}}\rvert^2$
# of constraints[1]	$\lvert\mathcal{K}\rvert + 3\lvert\mathcal{V}^{\mathtt{r}}\rvert + 3\lvert\mathcal{V}^{\mathtt{d}}\rvert + \lvert\mathcal{R}\rvert\lvert\mathcal{V}^{\mathtt{r}}\rvert + \lvert\mathcal{V}^{\mathtt{r}}\rvert\lvert\mathcal{K}\rvert + \lvert\mathcal{V}^{\mathtt{d}}\rvert\lvert\mathcal{V}^{\mathtt{r}}\rvert + \lvert\mathcal{V}^{\mathtt{d}}\rvert\lvert\mathcal{V}\rvert + \lvert\mathcal{V}^{\mathtt{r}}\rvert\lvert\mathcal{R}\rvert\lvert\mathcal{K}\rvert + \lvert\mathcal{V}^{\mathtt{r}}\rvert^2 + \lvert\mathcal{V}\rvert\lvert\mathcal{V}^{\mathtt{r}}\rvert^2 + 2\lvert\mathcal{R}\rvert\lvert\mathcal{V}^{\mathtt{r}}\rvert^2 + \lvert\mathcal{K}\rvert\lvert\mathcal{V}^{\mathtt{r}}\rvert^2 + \lvert\mathcal{K}\rvert\lvert\mathcal{R}\rvert\lvert\mathcal{V}^{\mathtt{r}}\rvert^2 + \lvert\mathcal{V}^{\mathtt{r}}\rvert^3$	$3\lvert\mathcal{V}^{\mathtt{d}}\rvert + 4\lvert\mathcal{V}^{\mathtt{r}}\rvert + \lvert\mathcal{V}^{\mathtt{d}}\rvert\lvert\mathcal{V}\rvert + 2\lvert\mathcal{V}^{\mathtt{r}}\rvert\lvert\mathcal{R}\rvert + \lvert\mathcal{V}^{\mathtt{d}}\rvert\lvert\mathcal{V}^{\mathtt{r}}\rvert + \lvert\mathcal{V}^{\mathtt{r}}\rvert\lvert\mathcal{R}\rvert\lvert\mathcal{K}\rvert + 4\lvert\mathcal{V}^{\mathtt{r}}\rvert^2 + \lvert\mathcal{V}\rvert\lvert\mathcal{V}^{\mathtt{r}}\rvert^2 + 3\lvert\mathcal{K}\rvert\lvert\mathcal{V}^{\mathtt{r}}\rvert^2 + \lvert\mathcal{R}\rvert\lvert\mathcal{V}^{\mathtt{r}}\rvert^2 + \lvert\mathcal{K}\rvert\lvert\mathcal{R}\rvert\lvert\mathcal{V}^{\mathtt{r}}\rvert^2 + \lvert\mathcal{V}^{\mathtt{r}}\rvert^3$	$3\lvert\mathcal{V}^{\mathtt{d}}\rvert + 7\lvert\mathcal{V}^{\mathtt{r}}\rvert + \lvert\mathcal{V}^{\mathtt{d}}\rvert\lvert\mathcal{V}^{\mathtt{r}}\rvert + \lvert\mathcal{V}^{\mathtt{d}}\rvert\lvert\mathcal{V}\rvert + 2\lvert\mathcal{V}^{\mathtt{r}}\rvert\lvert\mathcal{R}\rvert + \lvert\mathcal{V}^{\mathtt{r}}\rvert\lvert\mathcal{R}\rvert\lvert\mathcal{K}\rvert + (\lvert\mathcal{V}\rvert/2)(\lvert\mathcal{V}^{\mathtt{r}}\rvert^2 - \lvert\mathcal{V}^{\mathtt{r}}\rvert) + \lvert\mathcal{K}\rvert\lvert\mathcal{R}\rvert\lvert\mathcal{V}^{\mathtt{r}}\rvert^2 + 2\lvert\mathcal{V}^{\mathtt{r}}\rvert^2 + 3\lvert\mathcal{K}\rvert\lvert\mathcal{V}^{\mathtt{r}}\rvert^2 + \lvert\mathcal{R}\rvert\lvert\mathcal{V}^{\mathtt{r}}\rvert^2 + 2\lvert\mathcal{V}^{\mathtt{r}}\rvert^3$
# binary variables (and constraints) in an instance with $\lvert\mathcal{V}^{\mathtt{r}}\rvert = 1, \lvert\mathcal{V}^{\mathtt{d}}\rvert = 15, \lvert\mathcal{K}\rvert = 1, \lvert\mathcal{V}\rvert = 21$	38 (409)	39 (413)	18 (394)
# binary variables (and constraints) in an instance with $\lvert\mathcal{V}^{\mathtt{r}}\rvert = 29, \lvert\mathcal{V}^{\mathtt{d}}\rvert = 28, \lvert\mathcal{K}\rvert = 5, \lvert\mathcal{V}\rvert = 64$	741,762 (261,953)	80,011 (249,217)	52,171 (244,171)

[1] We approximate $\lvert\mathcal{V}^{\mathtt{r}}_0\rvert$ as $\lvert\mathcal{V}^{\mathtt{r}}\rvert$ and $\lvert\mathcal{R}\rvert - 1$ as $\lvert\mathcal{R}\rvert$ in the calculation of the number of variables and constraints.

MCSRP1 to MCSRP2 and from MCSRP2 to MCSRP3. Regarding the number of constraints, from MCSRP2 to MCSRP3, several constraints defined for $i > j$ were eliminated, but new constraints were also added. In general, a smaller number of constraints in MCSRP3 is expected compared to both MCSRP2 and MCSRP1. The computational results in Section 6.2 show that there is no model unrestrictedly recommended for all situations, e.g., some models are better to quickly return optimal solutions, whereas others are better to always find feasible solutions.

5 Properties and valid inequalities

In this section, we state a few properties of the problem and derive valid inequalities (VIs) based on them. We divide the VIs into two groups. In Section 5.1, we show the VIs related to the relief path decisions, while in Section 5.2, we present the VIs related to the crew scheduling and routing decisions. The VIs related to the relief path decisions are the same for the three models, while those related to routing decisions are specific for each model. For the sake of brevity, we detail only the VIs for MCSRP1 in this section. The VIs related to the routing decisions for the second and third formulations are presented in B.

5.1 VIs related to the relief path decisions

Multiple relief paths $0 - i$ may be available to reach a demand node i. Let $\mathcal{P}^{\mathtt{d}}_i$ be the set of possible $0 - i$ relief paths. We call E_p and $\mathcal{V}_p$ as the set of arcs and nodes used in path $p \in \mathcal{P}^{\mathtt{d}}_i$. Similarly, $\mathcal{V}^{\mathtt{r}}_p$ and $\mathcal{V}^{\mathtt{u}}_p$ are the set of damaged and undamaged nodes used in path $p \in \mathcal{P}^{\mathtt{d}}_i$. We define w_p as the sum of the length of the arcs used in path p, i.e., $w_p = \sum_{e \in E_p} \ell_e$. Since a relief path p connecting the depot with a demand node i must fall within a predefined maximum

distance $l_i^{\mathtt{d}}$, p is a feasible path if $w_p \leq l_i^{\mathtt{d}}$. This condition is valid, even if $l_i^{\mathtt{d}}$ is set as a sufficiently large number. We also define $\theta_{pi}^{\mathtt{d}}$ as the accessibility time of the demand node i if path p is selected to connect the depot with the demand node i and $\theta_j^{\mathtt{r}}$ as the restoration time of the damaged node j.

Given two paths p, $p' \in \mathcal{P}_i^{\mathtt{d}}$ such that $p \neq p'$, we say that p dominates p' if $\mathcal{V}_p^{\mathtt{r}} \subseteq \mathcal{V}_{p'}^{\mathtt{r}}$ and $w_p \leq l_i^{\mathtt{d}}$. In this case, p' is a dominated path. For special cases where $w_p \leq l_i^{\mathtt{d}}$, $w_{p'} \leq l_i^{\mathtt{d}}$ and $\mathcal{V}_p^{\mathtt{r}} = \mathcal{V}_{p'}^{\mathtt{r}}$ for $p \neq p'$, we can eliminate one of the paths, either p or p', from set $\mathcal{P}_i^{\mathtt{d}}$. We define $\mathcal{S}_i^{\mathtt{d}} \subseteq \mathcal{P}_i^{\mathtt{d}}$ as the set of nondominated paths from the depot to demand node i. Given that $\mathcal{S}_i^{\mathtt{d}}$ considers only nondominated paths, there are not two different paths using the same damaged nodes, i.e., $\mathcal{V}_p^{\mathtt{r}} \neq \mathcal{V}_{p'}^{\mathtt{r}}$ $\forall p, p' \in \mathcal{S}_i^{\mathtt{d}} : p \neq p'$. Finally, let $\mathcal{P}_i^{\mathtt{d}*} = \{p \in \mathcal{S}_i^{\mathtt{d}} \,|\, \mathcal{V}_p^{\mathtt{r}} = \emptyset\}$ be the set of nondominated paths that do not visit any damaged node and p_i^* be an element of set $\mathcal{P}_i^{\mathtt{d}*}$. Using the notation above, we state Propositions 1 and 2 as follows.

Proposition 1. *There is at least one optimal solution for MCSRP1 in which the paths used to connect the depot with the demand nodes are nondominated paths. Such a solution satisfies the following inequalities.*

$$|E_{p_i^*}| + |\mathcal{V}_{p_i^*}^{\mathtt{u}}| = \sum_{e \in E_{p_i^*}} Y_{ei} + \sum_{j \in \mathcal{V}_{p_i^*}^{\mathtt{u}}} V_{ji}, \forall\ i \in \mathcal{V}^{\mathtt{d}},\ p_i^* \in \mathcal{P}_i^{\mathtt{d}*} : \mathcal{P}_i^{\mathtt{d}*} \neq \emptyset, \tag{68}$$

$$(|E| + |\mathcal{V}|) \cdot (|\mathcal{V}_p^{\mathtt{r}}| - \sum_{j \in \mathcal{V}_p^{\mathtt{r}}} V_{ji}) \geq \sum_{e \in E \setminus E_p} Y_{ei} + \sum_{j \in \mathcal{V} \setminus \mathcal{V}_p} V_{ji}, \forall\ i \in \mathcal{V}^{\mathtt{d}}, p \in \mathcal{S}_i^{\mathtt{d}} : \mathcal{P}_i^{\mathtt{d}*} = \emptyset. \tag{69}$$

Proof. Let $p' \in \mathcal{P}_i^{\mathtt{d}}$ be a feasible dominated path and assume that p' is used to connect the depot to the demand node i. The accessibility time of node i depends on the restoration time of the damaged nodes in path p'. Then, $\theta_{p'i}^{\mathtt{d}} = \max_{j \in \mathcal{V}_{p'}^{\mathtt{r}}} \theta_j^{\mathtt{r}}$. Given that p' is a dominated path, there is one nondominated path p that dominates p', i.e., $\mathcal{V}_p^{\mathtt{r}} \subseteq \mathcal{V}_{p'}^{\mathtt{r}}$ and $w_p \leq l_i^{\mathtt{d}}$. Thus, p is also a feasible path. Furthermore, $\max_{j \in \mathcal{V}_p^{\mathtt{r}}} \theta_j^{\mathtt{r}} \leq \max_{j \in \mathcal{V}_{p'}^{\mathtt{r}}} \theta_j^{\mathtt{r}}$ since $\mathcal{V}_p^{\mathtt{r}} \subseteq \mathcal{V}_{p'}^{\mathtt{r}}$. Consequently, $\theta_{pi}^{\mathtt{d}} \leq \theta_{p'i}^{\mathtt{d}}$, and we can select p instead of p' without deteriorating the accessibility time of demand node i. The selection of the nondominated paths over dominated paths is imposed with inequalities (68) and (69). When there is a path p_i^*, this path is the only nondominated path to reach demand node i and can be fixed in the solution to MCSRP1 by using equations (68). If $\mathcal{P}_i^{\mathtt{d}*} \neq \emptyset$, the term $\sum_{j \in \mathcal{V}_p^{\mathtt{r}}} V_{ji} = |\mathcal{V}_p^{\mathtt{r}}|$ indicates that the damaged nodes of nondominated path p have been selected to reach demand node i, and inequalities (69) prohibit the selection of nodes and arcs that are not in the nondominated path p. □

Proposition 2. *If $\mathcal{P}_i^{\mathtt{d}*} = \emptyset$, the following inequalities can be added to MCSRP1 to set lower bounds for the accessibility time of the demand nodes:*

$$\sum_{j \in \mathcal{U}_i} V_{ji} \geq 1, \forall\ i \in \mathcal{V}^{\mathtt{d}} : \mathcal{P}_i^{\mathtt{d}*} = \emptyset, \tag{70}$$

$$Z_i^{\mathtt{d}} \geq \min_{k \in \mathcal{K}, j \in \mathcal{U}_i} (\rho_{k0j}^* + \delta_{kj}), \forall\ i \in \mathcal{V}^{\mathtt{d}} : \mathcal{P}_i^{\mathtt{d}*} = \emptyset, \tag{71}$$

$$\sum_{j \in n_i} V_{ji} = |n_i|, \forall\ i \in \mathcal{V}^{\mathtt{d}} : \mathcal{P}_i^{\mathtt{d}*} = \emptyset, \tag{72}$$

$$Z_i^{\mathtt{d}} \geq Z_j^{\mathtt{r}}, \forall\ j \in n_i, i \in \mathcal{V}^{\mathtt{d}} : \mathcal{P}_i^{\mathtt{d}*} = \emptyset, \tag{73}$$

$$Z_i^{\mathtt{d}} \geq \sum_{j \in \mathcal{V}^{\mathtt{r}}} \min_{\substack{k \in \mathcal{K}, l \in \mathcal{V}_0^{\mathtt{r}}: \\ l \neq j}} \left\{ \frac{\rho_{klj}^* + \delta_{kj}}{|\mathcal{K}|} \right\} \cdot V_{ji}, \forall\ i \in \mathcal{V}^{\mathtt{d}} : \mathcal{P}_i^{\mathtt{d}*} = \emptyset, \tag{74}$$

where ρ_{kij}^* is the shortest time for crew k to travel from node i to node j; $\mathcal{U}_i = \bigcup_{p \in \mathcal{S}_i^{\mathtt{d}}} \mathcal{V}_p^{\mathtt{r}}$ contains all the damaged nodes of the nondominated paths; and $n_i = \bigcap_{p \in \mathcal{S}_i^{\mathtt{d}}} \mathcal{V}_p^{\mathtt{r}}$ contains the damaged nodes that are used in all the nondominated paths.

Proof. If $\mathcal{P}_i^{\mathtt{d}*} = \emptyset$, it is clear that at least one damaged node j of the nondominated paths in $\mathcal{S}_i^{\mathtt{d}}$ must be used in the relief path $0 - i$ (inequalities (70)). In this case, some crew must arrive and repair such damaged node j. We know that to repair any damaged node j with a given crew k, the crew must arrive at node j consuming at least some travel time ρ_{k0j}^* and some repair time δ_{kj}. In this way, by selecting the minimum travel time plus the repair time to repair one of the damaged nodes of the nondominated paths in $\mathcal{S}_i^{\mathtt{d}}$, inequalities (71) establish a lower bound for the accessibility time of demand node i. If a node j exists in all the nondominated paths in set $\mathcal{S}_i^{\mathtt{d}}$, such node must be necessarily used in the relief paths $0 - i$ (inequalities (72)), and the demand node i does not become accessible before the restoration of such damaged node j (inequalities (73)). Finally, inequalities (74) state that all the damaged nodes that must be used in the paths from the depot to the demand node i should be repaired before node i becomes accessible. Given that we do not know the crew that will perform the restoration of each damaged node or the paths used by the crews in advance, we select the shortest repair time plus the travel time to arrive at the damaged nodes. Since any crew can be used to perform the restoration, the shortest time is divided by the number of crews. □

5.2 VIs related to the routing decisions

The VIs for the routing decisions are similar to those defined for the relief path decisions. We define $\mathcal{P}_{ij}^{\mathtt{r}}$ as the set of possible $i-j$ crew paths. Let $t_{kjp}^{\mathtt{v}}$ be the arrival time of crew k at damaged node $j \in \mathcal{V}_p^{\mathtt{r}}$ in path p; $t_{kjp}^{\mathtt{w}}$ be the waiting time of crew k at the damaged node $j \in \mathcal{V}_p^{\mathtt{r}}$ in path p; and t_{kp} be the total travel time of crew k in path p, i.e., $t_{kp} = \sum_{e \in E_p} \tau_{ke}$. We define $\mathcal{P}_{kij}^{\mathtt{r}*}$ (resp. $\mathcal{F}_{kij}^{\mathtt{r}*}$) as the set of paths with the shortest travel time between nodes i and j with crew k using (resp. not using) damaged nodes, i.e.,

$$\mathcal{P}_{kij}^{\mathtt{r}*} = \{p \in \mathcal{P}_{ij}^{\mathtt{r}} \,|t_{kp} \leq t_{kp'}, \forall p' \in \mathcal{P}_{ij}^{\mathtt{r}}\},\ \forall\ k \in \mathcal{K},\ i \in \mathcal{V}_0^r,\ j \in \mathcal{V}^r,$$

$$\mathcal{F}_{kij}^{\mathtt{r}*} = \{p \in \mathcal{P}_{ij}^{\mathtt{r}} \,|\, \mathcal{V}_p^{\mathtt{r}} = \emptyset\ , t_{kp} \leq t_{kp'}, \forall p' \in \mathcal{P}_{ij}^{\mathtt{r}} : \mathcal{V}_{p'}^{\mathtt{r}} = \emptyset\},\ \forall\ k \in \mathcal{K},\ i \in \mathcal{V}_0^r,\ j \in \mathcal{V}^r.$$

Given two paths $p', p \in \mathcal{P}_{ij}^{\mathtt{r}} : p \neq p'$, we say that p dominates p' for a crew k if $\mathcal{V}_p^{\mathtt{r}} \subseteq \mathcal{V}_{p'}^{\mathtt{r}}$ and $t_{kp} \leq t_{kp'}$. For cases where $\mathcal{V}_p^{\mathtt{r}} = \mathcal{V}_{p'}^{\mathtt{r}}$ and $t_{kp} = t_{kp'}$ for $p \neq p'$, we can eliminate one of the paths, either p or p', from set $\mathcal{P}_{ij}^{\mathtt{r}}$. We define $\mathcal{S}_{kij}^{\mathtt{r}} \subseteq \mathcal{P}_{ij}^{\mathtt{r}}$ as the set of nondominated paths from node i to node j using crew k. We also define $\mathcal{D}_p$ as the set of paths using nodes of set $\mathcal{V}_p^{\mathtt{r}}$ that are not

dominated by p. In this way,

$$\mathcal{D}_p = \{p' \in \mathcal{S}^{\mathtt{r}}_{kij} | \mathcal{V}^{\mathtt{r}}_p \subseteq \mathcal{V}^{\mathtt{r}}_{p'}, t_{kp} \geq t_{kp'}\}, \forall p \in \mathcal{S}^{\mathtt{r}}_{kij},\ k \in \mathcal{K},\ i \in \mathcal{V}^{\mathtt{r}}_0,\ j \in \mathcal{V}^{\mathtt{r}}.$$

Let p^*_{kij} and f^*_{kij} be the elements of sets $\mathcal{P}^{\mathtt{r}*}_{kij}$ and $\mathcal{F}^{\mathtt{r}*}_{kij}$, respectively. Additionally, we define h_p as the hth damaged node visited in path p, for $h = 1, ..., H$, where $H = |\mathcal{V}^{\mathtt{r}}_p|$. In this way, H_p denotes the last damaged node visited in path p. Let ρ_{kij} be the shortest travel time required for crew k to travel from node i to node j without using damaged nodes. Based on this notation, we state Propositions 3 and 4, which assume that crew k can repair both nodes i and j.

Proposition 3. *There is at least one optimal solution for MCSRP1 in which the paths used by crew k to travel from node i to node j are nondominated paths, where i and j are consecutive nodes in the schedule of crew k, i.e., $X_{kij} = 1$. Such a solution satisfies the following inequalities:*

$$\sum_{e \in E_{f^*_{kij}}} P_{eij} + \sum_{l \in \mathcal{V}^{\mathtt{u}}_{f^*_{kij}}} N^{\mathtt{u}}_{lij} \geq (|E_{f^*_{kij}}| + |\mathcal{V}^{\mathtt{u}}_{f^*_{kij}}|) \cdot X_{kij}, \forall k \in \mathcal{K}, i \in \mathcal{V}^{\mathtt{r}}_0, j \in \mathcal{V}^{\mathtt{r}} : \mathcal{F}^{\mathtt{r}*}_{kij} \neq \emptyset, t_{kf^*_{kij}} = t_{kp^*_{kij}}, \tag{75}$$

$$(|E| + |\mathcal{V}|) \cdot (1 + |\mathcal{V}^{\mathtt{r}}_p| - X_{kij} - \sum_{h \in \mathcal{R}} \sum_{l \in \mathcal{V}^{\mathtt{r}}_p} N^{\mathtt{r}}_{lhij}) \geq \sum_{e \in E \setminus \bigcup_{p' \in \mathcal{D}_p} E_{p'}} P_{eij} + \sum_{l \in \mathcal{V} \setminus \bigcup_{p' \in \mathcal{D}_p} \mathcal{V}_{p'}} N^{\mathtt{u}}_{lij},$$

$$\forall\ k \in \mathcal{K},\ i \in \mathcal{V}^{\mathtt{r}}_0,\ j \in \mathcal{V}^{\mathtt{r}},\ p \in \mathcal{S}^{\mathtt{r}}_{kij} : (\mathcal{F}^{\mathtt{r}*}_{kij} = \emptyset) \vee (\mathcal{F}^{\mathtt{r}*}_{kij} \neq \emptyset, p \neq f^*_{kij}, t_{kf^*_{kij}} > t_{kp^*_{kij}}). \tag{76}$$

Proof. We need to prove that given a dominated path p', we can replace it by a nondominated path p without increasing the restoration time of damaged node j. According to constraints (3) and (4), the restoration time $\theta^{\mathtt{r}}_j$ of node j repaired by a given crew k that uses path p as crew path $i - j$ is calculated as $\theta^{\mathtt{r}}_j = \theta^{\mathtt{r}}_i + t_{kp} + \delta_{kj}$ if $\mathcal{V}^{\mathtt{r}}_p = \emptyset$, and $\theta^{\mathtt{r}}_j = \max\{\theta^{\mathtt{r}}_i + t_{kp} + \delta_{kj}, t^{\mathtt{w}}_{kH_pp} + t^{\mathtt{v}}_{kH_pp} + \rho_{kH_pj} + \delta_{kj}\}$ if $\mathcal{V}^{\mathtt{r}}_p \neq \emptyset$. We focus on the case with $\mathcal{V}^{\mathtt{r}}_p \neq \emptyset$, and the development for the other case follows similarly. The arrival time $t^{\mathtt{v}}_{kh_pp}$ at the hth damaged node in path p can be computed as $t^{\mathtt{v}}_{kh_pp} = t^{\mathtt{v}}_{k(h-1)_pp} + t^{\mathtt{w}}_{k(h-1)_pp} + \rho_{k(h-1)_ph_p}$. Then, recursively, $t^{\mathtt{v}}_{kH_pp}$ can be evaluated as

$$t^{\mathtt{v}}_{kH_pp} = \sum_{h'=1}^{h'=H-1} t^{\mathtt{w}}_{k(h')_pp} + \sum_{h'=1}^{h'=H-1} \rho_{k(h')_p(h'+1)_p} + \rho_{ki1_p} + \theta^{\mathtt{r}}_i.$$

Then,

$$t^{\mathtt{w}}_{kH_pp} + t^{\mathtt{v}}_{kH_pp} + \rho_{kH_pj} = t^{\mathtt{w}}_{kH_pp} + \sum_{h'=1}^{h'=H-1} t^{\mathtt{w}}_{k(h')_pp} + \sum_{h'=1}^{h'=H-1} \rho_{k(h')_p(h'+1)_p} + \rho_{ki1_p} + \theta^{\mathtt{r}}_i + \rho_{kH_pj}.$$

Grouping similar terms, we obtain

$$t^{\mathtt{w}}_{kH_pp} + t^{\mathtt{v}}_{kH_pp} + \rho_{kH_pj} = \sum_{h'=1}^{h'=H} t^{\mathtt{w}}_{k(h')_pp} + t_{kp} + \theta^{\mathtt{r}}_i = \sum_{l \in \mathcal{V}^{\mathtt{r}}_p} t^{\mathtt{w}}_{klp} + t_{kp} + \theta^{\mathtt{r}}_i,$$

in which $t_{kp} = \sum_{h'=1}^{h'=H-1} \rho_{k(h')_p(h'+1)_p} + \rho_{ki1_p} + \rho_{kH_pj}$. Therefore, the calculation of $\theta^{\mathtt{r}}_j$ can be

expressed as

$$\theta_j^{\mathtt{r}} = \max\{\theta_i^{\mathtt{r}} + t_{kp} + \delta_{kj}, \sum_{l \in \mathcal{V}_p^{\mathtt{r}}} t_{klp}^{\mathtt{w}} + t_{kp} + \theta_i^{\mathtt{r}} + \delta_{kj}\}. \tag{77}$$

Now, let us consider a path p' dominated by a nondominated path p. We have $t_{kp} \leq t_{kp'}$ according to the definition. Then, $\theta_i^{\mathtt{r}} + t_{kp} + \delta_{kj} \leq \theta_i^{\mathtt{r}} + t_{kp'} + \delta_{kj}$. Additionally, since $\mathcal{V}_p^{\mathtt{r}} \subseteq \mathcal{V}_{p'}^{\mathtt{r}}$, the use of path p' implies waiting for the restoration of the nodes that belong to set $\mathcal{V}_p^{\mathtt{r}}$ and waiting for the restoration of additional damaged nodes that belong to $\mathcal{V}_{p'}^{\mathtt{r}} \setminus \mathcal{V}_p^{\mathtt{r}}$. Therefore, $\sum_{l \in \mathcal{V}_p^{\mathtt{r}}} t_{klp}^{\mathtt{w}} + t_{kp} + \theta_i^{\mathtt{r}} + \delta_{kj} \leq \sum_{l \in \mathcal{V}_{p'}^{\mathtt{r}}} t_{klp'}^{\mathtt{w}} + t_{kp'} + \theta_i^{\mathtt{r}} + \delta_{kj}$. Consequently, we can use p instead of p' without increasing the restoration time of node j. Inequalities (75)-(76) are analogous to inequalities (68)-(69) to force the selection of a nondominated path over dominated paths. If $\mathcal{F}_{kij}^{\mathtt{r}*} \neq \emptyset$ and $t_{kp_{kij}^*} = t_{kf_{kij}^*}$, f_{kij}^* is the only nondominated path in set $\mathcal{S}_{kij}^{\mathtt{r}}$ and can be fixed in the solution to MCSRP1 with equations (75) if $X_{kij} = 1$. Inequalities (76) prevent the selection of dominated paths over nondominated paths. If path p is a nondominated path and the damaged nodes of path p are used to travel from node i to node j ($\sum_{h \in \mathcal{R}} \sum_{l \in \mathcal{V}_p^{\mathtt{r}}} N_{lhij}^{\mathtt{r}} = |\mathcal{V}_p^{\mathtt{r}}|$), inequalities (76) prohibit the use of a path dominated by path p if $\mathcal{F}_{kij}^{\mathtt{r}*} = \emptyset$ or if $\mathcal{F}_{kij}^{\mathtt{r}*} \neq \emptyset, p \neq f_{kij}^*$ and $t_{kf_{kij}^*} > t_{kp_{kij}^*}$. □

Proposition 4. *The following inequalities can be added to MCSRP1 to set lower bounds for the restoration time of the damaged nodes.*

$$Z_j^{\mathtt{r}} \geq (t_{kp_{k0j}^*} + \delta_{kj}) \cdot X_{k0j} + \sum_{i \in \mathcal{V}^{\mathtt{r}}} ((t_{kp_{k0i}^*} + \delta_{ki} + t_{kp_{kij}^*} + \delta_{kj}) \cdot X_{kij}), \forall\, k \in \mathcal{K},\ j \in \mathcal{V}^{\mathtt{r}}, \tag{78}$$

$$Z_j^{\mathtt{r}} \geq Z_i^{\mathtt{r}} + t_{kp_{kij}^*} + \delta_{kj} - M \cdot (1 - X_{kij}), \forall\, k \in \mathcal{K},\ i \in \mathcal{V}_0^{\mathtt{r}},\ j \in \mathcal{V}^{\mathtt{r}}. \tag{79}$$

Proof. Inequalities (78) are based on the fact that any damaged node j considered in the schedule of a given crew k must be reached by it using some path p. Although path p is unknown, if j is the first node in the schedule of crew k ($X_{k0j} = 1$), $t_{kp_{k0j}^*}$ can be used as a lower bound for the travel time in this path. Furthermore, if j is not the first node in the schedule of crew k, this crew must spend additional time to arrive and repair some node i ($t_{kp_{k0i}^*} + \delta_{ki}$) before traveling to node j. Inequalities (79) are similar to constraints (3) replacing the term $\sum_{e \in E} \tau_{ke} \cdot P_{eij}$ with a lower bound for the travel time between nodes i and j ($t_{kp_{kij}^*}$). □

The number of nodes in set $\mathcal{R}$ can be redefined for each pair of nodes i and j based on the number of damaged nodes of the nondominated paths. Thus, instead of $\mathcal{R}$, we can use a set $\mathcal{R}_{ij}$ defined as follows:

$$\mathcal{R}_{ij} = \{1, ..., \max_{p \in \mathcal{S}_{kij}^{\mathtt{r}}, k \in \mathcal{K}} |\mathcal{V}_p^{\mathtt{r}}|\}.$$

This redefinition of $\mathcal{R}$ can drastically reduce the number of variables depending on the position h because the use of fewer damaged nodes in the nondominated paths is expected.

5.3 Separation algorithms for the VIs

To generate the VIs related to relief path decisions, we need the estimation of sets $\mathcal{U}_i, \mathcal{P}_i^{\mathtt{d}*}, n_i$, and $\mathcal{S}_i^{\mathtt{d}}$. Analogously, to generate the VIs related to routing decisions, we need to estimate sets $\mathcal{P}_{kij}^{\mathtt{r}*}, \mathcal{F}_{kij}^{\mathtt{r}*}$, and $\mathcal{S}_{kij}^{\mathtt{r}}$. $\mathcal{P}_i^{\mathtt{d}*}, n_i, \mathcal{P}_{kij}^{\mathtt{r}*}$, and $\mathcal{F}_{kij}^{\mathtt{r}*}$ can be estimated by separation algorithms based on the shortest path problem (SPP) and executed before solving the optimization models. For instance, $\mathcal{P}_{kij}^{\mathtt{r}*}$ is found by solving the SPP between damaged nodes i and j over the original graph G. Additionally, $\mathcal{F}_{kij}^{\mathtt{r}*}$ is evaluated by solving the SPP between damaged nodes i and j over a graph G', in which the damaged nodes $l \in \mathcal{V}^r : l \neq i, l \neq j$ and the arcs incident to them are removed. Similarly, $\mathcal{P}_i^{\mathtt{d}*}$ is determined by solving the SPP between the depot and demand node i over the same graph G'. Set n_i can be determined by solving one SPP for each damaged node $l \in \mathcal{V}^r$. Basically, to know if a damaged node l is an element of n_i, we remove node l and its incident arcs from graph G, and the SPP between the depot and demand node i is solved. If there is a path from the depot to demand node i with a cost less than or equal to $l_i^{\mathtt{d}}$, node l is not an element of n_i. Otherwise, we insert node l into n_i. Set n_i can also be found as $n_i = \bigcap_{p \in \mathcal{S}_i^{\mathtt{d}}} \mathcal{V}_p^{\mathtt{r}}$ if set $\mathcal{S}_i^{\mathtt{d}}$ is available. In E, we detail the separation algorithms used to generate sets $\mathcal{P}_i^{\mathtt{d}*}, \mathcal{P}_{kij}^{\mathtt{r}*}, \mathcal{F}_{kij}^{\mathtt{r}*}$, and n_i.

The estimation of $\mathcal{U}_i, \mathcal{S}_i^{\mathtt{d}}$ and $\mathcal{S}_{kij}^{\mathtt{r}}$ is not trivial and may require the development of specialized algorithms that are not the focus here. Thus, we approximate these sets in such a way to maintain the inequalities valid, although they might be weaker. For instance, instead of considering all the nondominated paths in $\mathcal{S}_{kij}^{\mathtt{r}}$, we consider a subset $\widehat{\mathcal{S}}_{kij}^{\mathtt{r}} \subseteq \mathcal{S}_{kij}^{\mathtt{r}}$ with some nondominated paths. The algorithm used to find subset $\widehat{\mathcal{S}}_{kij}^{\mathtt{r}}$ is outlined in Algorithm 1. First, we find the shortest path p from the depot to demand node i considering the original graph G. Path p is a nondominated path since it is the path with the smallest t_{kp}. Then, we remove the damaged nodes $\mathcal{V}_p^r$ used in path p from graph G, and the SPP is solved again. The new path p' is a path that is nondominated by p because it uses different damaged nodes. Furthermore, p' is the shortest path using nodes $\mathcal{V}_{p'}^r$ and dominates other paths using such nodes but at a higher cost. The process is repeated iteratively until the shortest path algorithm cannot find more paths that are feasible. A similar idea can be used to find $\widehat{\mathcal{S}}_i^{\mathtt{d}}$.

Algorithm 1 Algorithm to find the set $\widehat{\mathcal{S}}^{\mathtt{r}}_{kij}$.

`Input:`
Graph $G = (\mathcal{V}, E)$; Indices i, j, k; Parameter τ_{ke}, $\forall e \in E$;
`Output:`
Paths $p \in \widehat{\mathcal{S}}^{\mathtt{r}}_{kij}$;

`Initialization`:
$t_{kp} := 0$;
while $t_{kp} < +\infty$ **do**
    Find the shortest path p from node i to node j;
    if path p exists **then**
        $t_{kp} := \sum_{e \in E_p} \tau_{ke}$;
        Save path p in set $\widehat{\mathcal{S}}^{\mathtt{r}}_{kij}$;
        Remove nodes in $\mathcal{V}^r_p$ and the arcs incident to them from graph G;
    else
        $t_{kp} := +\infty$;
    end if
end while
return set $\widehat{\mathcal{S}}^{\mathtt{r}}_{kij}$;

Set $\mathcal{U}_i$ is simply considered as $\mathcal{U}_i = \mathcal{V}^r$, which maintains the validity of the inequalities involving $\mathcal{U}_i$. Finally, since we do not have the exact set $\mathcal{S}^{\mathtt{r}}_{kij}$, $\mathcal{R}_{ij}$ is approximated as follows:

$$\mathcal{R}_{ij} = \{1, ..., \max_{p \in \mathcal{P}^{\mathtt{r}}_{ij}} |\mathcal{V}^{\mathtt{r}}_p|\},$$

where $\max_{p \in \mathcal{P}^{\mathtt{r}}_{ij}} |\mathcal{V}^{\mathtt{r}}_p|$ is equal to the number of nodes in the path with more damaged nodes in $\mathcal{P}^{\mathtt{r}}_{ij}$. Such a calculation can be performed with an algorithm to find the elementary longest path (the one with more damaged nodes) from node i to node j. We use an integer linear programming model from the literature (Bui et al., 2016) to find such a path.

6 Computational results

The goal of this section is twofold: first, to compare the performance of the proposed formulations and valid inequalities (Section 6.2); second, to analyze the solutions of the problem in a practical case based on a real-world natural disaster (Section 6.3). From this analysis, we illustrate the implication of the multiple crews in the problem and provide managerial insights that might be useful in practice. All the algorithms were coded in the C++ programming language and run on a PC with an AMD Opteron 6172 processor with 16.0 GB of RAM and a single thread. The MIP models were solved by the IBM CPLEX Optimization Solver 12.8. To avoid running out of memory, we allow CPLEX to store the branch-and-bound tree in a file. The stopping criterion was either the elapsed time exceeding the time limit of 3,600 seconds or the optimality gap being smaller than 10^{-4}. All the remaining parameters of CPLEX were kept at their default values.

6.1 Instance and experiment description

The models were tested using two different sets of instances. The first set (set L) is derived from the benchmark instances for the SCSRP. We selected the first 12 classes of instances used

in Maya-Duque et al. (2016) and Moreno et al. (2019). Originally, the instances were proposed by Maya-Duque et al. (2016) considering different proportions of damaged arcs in randomly generated networks. For each damaged arc, the authors included one or more damaged nodes in the middle of some arcs. For each class, we consider 12 instances. The second set of instances (set CS) is based on a real network affected by a disaster in the State of Rio de Janeiro in Brazil. This disaster has been studied before in the literature (Alem et al., 2016; Moreno et al., 2016, 2018) but with a different focus. The authors considered some damaged arcs along the network for different disaster scenarios, but they did not focus on the restoration of such arcs. Six main highways and 13 main cities were affected by this disaster. Although the highways may have been affected in more than one point, we consider some instances assuming one damaged node in each one of the affected highways. Additionally, we generated instances based on the original network of the disaster but randomly selected the location of the damaged nodes. In this respect, we generate instances with 6, 10 and 14 damaged nodes. Further details on the instance generation are provided in C.

Repair and travel times for the multiple crews were generated based on the literature (Taillard, 1999). They are stated as $\tau_{ke} = \alpha_k^1 \tau'_e$ and $\delta_{kj} = \alpha_k^2 \delta'_j$, where α_k^1 and α_k^2 are travel and repair factors randomly generated either in the interval [0.4, 1.0] or in the interval [1.0, 2.0], while δ'_j and τ'_e are the repair and travel times in the SCSRP, respectively. We generate the velocity factors in such a way that no single crew is much better or worse than the others. We also consider that the crews with heavier machinery may perform a faster restoration but may spend more time arriving at the damaged nodes. Thus, the crew with a travel factor generated in the interval [0.4, 1.0] has a repair factor generated in the interval [1.0, 2.0], and vice versa. Table 3 shows the main characteristics of the proposed instances. The first crew has factors $\alpha_1^1 = \alpha_1^2 = 1.0$. In this way, we keep the travel and repair times of this crew as those used in the SCSRP. Additionally, the crews have different factors over the classes of instances. There are 144 instances from the literature and 114 instances based on the real-world case. We run experiments with 1, 3 and 5 crews, totaling 774 instances.

Table 3: Set of instances.

Instance class	Travel (repair) factors of the crews[1]					Demand nodes	Damaged nodes	Total nodes	Total arcs	Total instances
	Crew 1	Crew 2	Crew 3	Crew 4	Crew 5					
L1	1.0 (1.0)	0.7 (1.2)	1.5 (0.7)	0.7 (1.3)	1.8 (0.9)	15	1 to 9	21 to 29	40 to 48	12
L2	1.0 (1.0)	0.7 (1.9)	1.7 (0.6)	0.9 (1.7)	1.3 (0.8)	15	1 to 9	21 to 29	38 to 46	12
L3	1.0 (1.0)	0.6 (2.0)	1.1 (0.4)	0.7 (1.6)	1.3 (0.9)	15	1 to 9	21 to 29	38 to 46	12
L4	1.0 (1.0)	0.7 (1.8)	1.6 (0.9)	0.9 (1.4)	1.6 (0.9)	19	2 to 10	27 to 35	42 to 50	12
L5	1.0 (1.0)	0.9 (1.8)	1.1 (0.6)	0.7 (1.8)	1.4 (0.6)	19	1 to 9	26 to 34	38 to 48	12
L6	1.0 (1.0)	0.8 (1.7)	1.8 (0.4)	0.5 (2.0)	1.8 (0.9)	19	1 to 9	26 to 34	40 to 48	12
L7	1.0 (1.0)	0.4 (1.9)	1.7 (0.6)	0.8 (1.6)	1.1 (0.8)	24	4 to 20	34 to 50	87 to 103	12
L8	1.0 (1.0)	0.8 (1.7)	1.4 (0.9)	0.7 (1.1)	1.6 (0.6)	24	4 to 22	34 to 52	93 to 111	12
L9	1.0 (1.0)	0.7 (1.5)	1.7 (0.9)	0.8 (1.9)	1.9 (0.5)	24	4 to 21	34 to 51	88 to 105	12
L10	1.0 (1.0)	0.7 (1.4)	1.4 (0.8)	0.6 (1.1)	1.4 (0.6)	28	5 to 29	40 to 64	123 to 147	12
L11	1.0 (1.0)	0.6 (1.3)	1.3 (0.5)	0.8 (1.1)	1.2 (0.9)	28	5 to 28	40 to 63	120 to 143	12
L12	1.0 (1.0)	0.5 (1.4)	1.6 (0.5)	0.9 (2.0)	1.8 (0.4)	28	5 to 28	40 to 63	118 to 141	12
CS0	1.0 (1.0)	0.7 (1.2)	1.5 (0.7)	0.7 (1.3)	1.8 (0.9)	13	6	66	95	6
CS1	1.0 (1.0)	0.7 (1.2)	1.5 (0.7)	0.7 (1.3)	1.8 (0.9)	13	6 to 14	66 to 74	95 to 103	18
CS2	1.0 (1.0)	0.7 (1.9)	1.7 (0.6)	0.9 (1.7)	1.3 (0.8)	13	6 to 14	66 to 74	95 to 103	18
CS3	1.0 (1.0)	0.6 (2.0)	1.1 (0.4)	0.7 (1.6)	1.3 (0.9)	13	6 to 14	66 to 74	95 to 103	18
CS4	1.0 (1.0)	0.7 (1.8)	1.6 (0.9)	0.9 (1.4)	1.6 (0.9)	20	6 to 14	66 to 74	95 to 103	18
CS5	1.0 (1.0)	0.9 (1.8)	1.1 (0.6)	0.7 (1.8)	1.4 (0.6)	20	6 to 14	66 to 74	95 to 103	18
CS6	1.0 (1.0)	0.8 (1.7)	1.8 (0.4)	0.5 (2.0)	1.8 (0.9)	20	6 to 14	66 to 74	95 to 103	18
Total										$258 \cdot 3 = 774$

[1] Values for $\alpha_k^1(\alpha_k^2)$. For instances with $|\mathcal{K}| < 5$ consider the first $|\mathcal{K}|$ crews.

The computational experiments considering the proposed models and valid inequalities were conducted in four phases, as presented in Table 4. First, we run the three formulations without including any valid inequality. Second, we run them all but include all the devised valid inequalities. Third, we run only formulation MCSRP3 with some of the VIs. The objective is to verify the impact of the different types of VIs on the performance of the formulations. In this respect, VIs were divided into four groups: (VIs1) VIs to set lower bounds for variables $Z_i^{\mathtt{d}}$ and V_{ji}; (VIs2) VIs to impose and select nondominated relief paths over dominated relief paths; (VIs3) VIs to set lower bounds for variables $Z_i^{\mathtt{r}}$; (VIs4) VIs to impose and select nondominated crew paths over dominated crew paths. Finally, we apply the graph reduction strategy proposed by Moreno et al. (2019) to improve the performance of the MRRP3+VIs approach. The graph reduction consists of solving the problem over a graph with a reduced number of nodes, thus deriving lower bounds for the variables of the original problem. It relies on the elimination of intersection nodes and arcs that are not directly connected to either damaged or demand nodes. The reduced graph is commonly built by splitting the set of damaged nodes into subsets according to an initial solution. Since we do not resort to trivial initial solutions, the damaged nodes are labeled from 1 to $|\mathcal{V}^r|$, and the subsets are built by selecting the nodes in increasing order of the label. We consider reduced graphs with 4 damaged nodes, which can be easily solved by the proposed formulations. A description of the graph reduction strategy is presented in D.

Table 4: Solution strategies.

Strategy	Description
MCSRP1	First MCSRP formulation.
MCSRP2	Second MCSRP formulation.
MCSRP3	Third MCSRP formulation.
MCSRP1+VIs	First MCSRP formulation + all VIs.
MCSRP2+VIs	Second MCSRP formulation + all VIs.
MCSRP3+VIs	Third MCSRP formulation + all VIs.
MCSRP3+VIs1	Third MCSRP formulation + VIs (70)-(74).
MCSRP3+VIs2	Third MCSRP formulation + VIs (68),(69).
MCSRP3+VIs3	Third MCSRP formulation + VIs (84),(85).
MCSRP3+VIs4	Third MCSRP formulation + VIs (86)-(89).
MCSRP3+VIs*	Third MCSRP formulation + all VIs + graph reduction.

6.2 Computational performance of the mathematical formulations

In this section, we analyze the computational performance of the proposed models and valid inequalities. First, we compare the three MCSRP formulations (MCSRP1, MCSRP2, MCSRP3) with and without the VIs. Figure 3 presents the performance profiles (Dolan and Moré, 2002) for the MCSRP models based on the optimality gap for the considered instances. The optimality gap is computed as $gap = \frac{Z^U - Z^L}{Z^U}$, in which Z^U is the upper bound or cost of the best integer solution and Z^L is the lower bound. Given a set $\mathcal{P}$ of instances and a set $\mathcal{F}$ of solution methods, let gap_{fp} be the gap of the solution of instance p solved by method f. The value $P(f,q)$ (y-axis) when $q > 0$ (x-axis) indicates the fraction of instances for which a strategy f provides solutions with a gap within a factor of 2^q of the best obtained gap, i.e., the fraction of instances for which $gap_{fp} + \epsilon \leq 2^q \cdot \min_{f' \in \mathcal{F}} \{gap_{f'p} + \epsilon\}$, where $\epsilon = 0.01$ is a near-zero value. The value of $P(f,q)$ when $q = 0$ is the fraction of instances for which the strategy f reached the best

gap. For example, the red asterisk (*) in Figure 3 indicates that for 92% of the instances, strategy MCSRP1+VIs provides solutions with gaps within a factor of $2^{0.54}$ (1.45) of the best gap. Indeed, $gap_{fp}+\epsilon \leq 1.45 \cdot \min_{f' \in \mathcal{F}} \{gap_{f'p}+\epsilon\}$ for 92% of the instances, with f = MCSRP1+VIs and F = {MCSRP1, MCSRP2, MCSRP3, MCSRP1+VIs, MCSRP2+VIs, MCSRP3+VIs}.

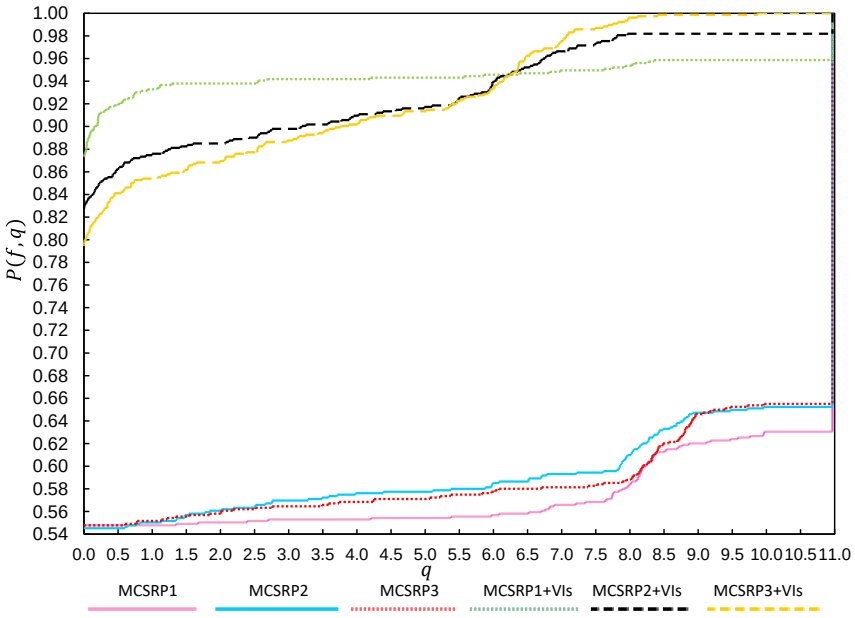

Figure 3: Performance profiles based on gap for the MCSRP formulations.

Note that the VIs significantly improve the computational performance of the three formulations. Without the VIs, models MCSRP1, MCSRP2, and MCSRP3 find the best gap for 54.65%, 54.39%, and 54.52% of the instances, respectively. When the inequalities are included, the percentage of instances with the best gap increases to 86.69%, 82.04%, and 79.32%, respectively. With the VIs, model MCSRP1 demonstrates good performance in approximately 92% of the considered cases, but it presents the worst convergence when all the instances are considered. MCSRP2+VIs and MCSRP3+VIs showed a more stable convergence, even though they achieved the best gap for a smaller number of instances when compared to MCSRP1+VIs. MCSRP3 outperformed MCSRP2, both with and without the VIs.

Table 5 shows the number and percentage of instances for which CPLEX found feasible solutions (#feas, %feas), the number and percentage of instances that CPLEX solved to optimality (#opt, %opt), the average elapsed time in seconds (Avg. time), and the average number of nodes processed in the branch-and-cut tree (nodes B&C). Tables 9 and 10 in F present additional results of the three models with and without the VIs for instances with different numbers of crews. For all models, the elapsed time is significantly reduced by the VIs. On average, for model MCSRP1 (MCSRP2, MCSRP3) the elapsed time is reduced by 51.82% (51.30%, 41.42%) in set L and 52.05% (29.52%, 23.80%) in set CS. The impact of the VIs is more pronounced in the CS instances. For example, the number of instances solved to optimality with model MCSRP3 in set CS increased 80.87% with the VIs, while in set L, it increased 18.36%.

In both sets of instances, L and CS, MCSRP1 outperformed MCSRP2 and MCSRP3 regarding the number of optimal solutions, but it had difficulty in finding feasible solutions in

Table 5: Average results of the MCSRP formulations.

Solution method	Set L (432 instances)					Set CS (342 instances)					Nodes B&C[1]
	#feas	%feas	#opt	%opt	Avg. time (seconds)	#feas	%feas	#opt	%opt	Avg. time (seconds)	
MCSRP1	365	84.49	316	73.15	1,065	121	35.38	113	33.04	2,427	24,078
MCSRP2	379	87.73	300	69.44	1,170	126	36.84	113	33.04	2,372	30,950
MCSRP3	381	88.19	305	70.60	1,151	126	36.84	115	33.63	2,362	17,566
MCSRP1+VIs	426	98.61	376	87.04	512	316	92.40	242	70.76	1,194	10,571
MCSRP2+VIs	432	100.00	373	86.34	570	328	95.91	209	61.11	1,590	26,020
MCSRP3+VIs	432	100.00	361	83.56	674	342	100.00	208	60.82	1,718	68,565

[1] Values based on the feasible solutions. Values for MCSRP1, MCSRP2, and MCSRP3 are not representative.

more cases. Eliminating some symmetric solutions in the third formulation was effective in finding feasible solutions for all the considered instances within the time limit, but the number of solutions that proved optimal was smaller than in MCSRP1+VIs. The effectiveness of MCSRP3+VIs in finding feasible solutions appeared to be related to the number of nodes that can be processed in the B&C tree, which is significantly higher when solving MCSRP3+VIs compared to the other two formulations. For the instances based on the real-world disaster aftermath (set CS), model MCSRP1+VIs is 30.54% faster than MCSRP3+VIs and solves 14.05% more instances to optimality, although it fails to find feasible solutions in 7.6% of the cases. In contrast, MCSRP3+VIs finds feasible solutions for all CS instances. Evidently, there is a trade-off that can be explored in practical situations according to preferences or necessities of the decision-maker. On the one hand, MCSRP1+VIs is better at finding optimal solutions for some instances quickly, while it struggles to find feasible solutions in some other instances. On the other hand, MCSRP3+VIs always finds feasible solutions (many good-quality ones), but optimality certificate is slightly compromised. The second model presents a balance between the first and the third models. Regarding MCSRP1+VIs, MCSRP2+VIs returns more feasible solutions at the expenses of increased computational times, and fewer solutions proven optimal; whereas regarding MCSRP3+VIs, MCSRP2+VIs is faster and provides more optimal solutions, even though it finds fewer feasible solutions.

Figure 4 presents the performance profiles based on the optimality gap to compare how the different valid inequalities affect the performance of MCSRP3. The impact of the different VIs in the performance of models MCSRP1 and MCSRP2 is similar. Notice that the performance profiles did not converge to $P(f, q) = 1$, indicating that none of the compared strategies could find feasible solutions for all the considered instances. The VIs with the highest impact on the gap of the solutions are those used to impose and select nondominated relief paths over dominated relief paths (VIs2), which found feasible solutions in 98.71% of the cases. The fraction of instances solved with the best gap increased from approximately 60% to 88% when the VIs2 were included. The VIs4, whose goal is to impose and select nondominated crew paths over dominated crew paths, also had a relevant impact on the gap. VIs2 and VIs4 helped to significantly reduce the number of solutions that needed to be explored by cutting off solutions with nondominated paths. VIs1 and VIs3 helped to improve the linear relaxation of the problem by setting lower bounds for the accessibility ($Z_i^{\mathtt{d}}$) and restoration ($Z_j^{\mathtt{r}}$) time. VIs1 had a more pronounced impact than VIs3 because the accessibility time is directly penalized in the objective function, while the restoration time of a given damaged node i does not directly affect the cost of the problem if

node i is not considered in some relief path.

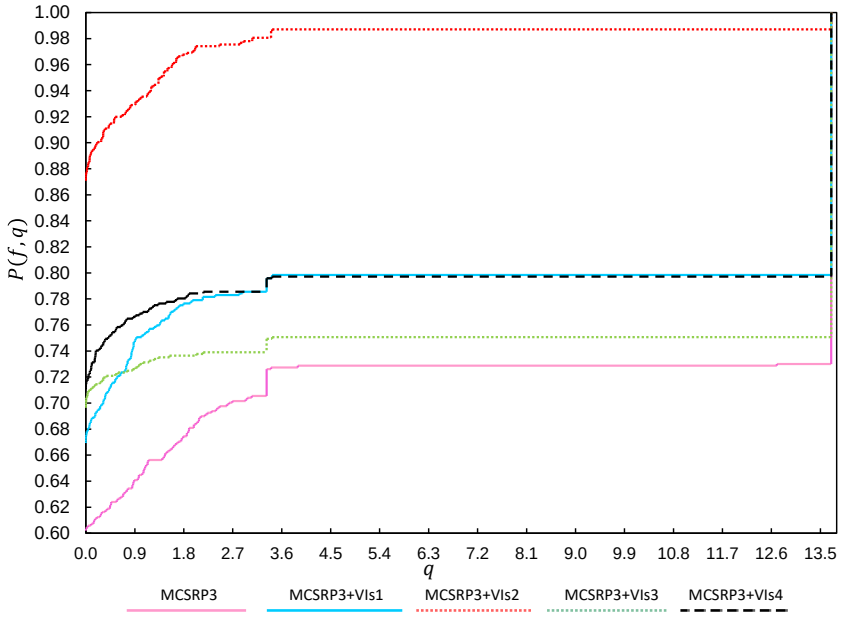

Figure 4: Performance profiles based on gap for the model MCSRP3 with different type of VIs.

Table 6 compares the average results of MCSRP3+VIs and the same strategy applying the graph reduction strategy (MCSRP3+VIs*). Additional results of the MCSRP3+VIs and MCSRP3+VIs* are presented in Tables 11 and 12 in F. The graph reduction strategy improved the average upper, lower bound and gap of the solutions. The average gap was reduced from 5.75% to 3.45% for L instances and from 9.70% to 4.71% for CS instances. The average elapsed time was slightly longer when the graph reduction strategy was applied because of the prepossessing step required to reduce and solve the reduced graphs. On average, the instances based on the real case were harder to solve than the instances from the literature. The average time, for example, was 719 seconds with the MCSRP3+VIs* strategy for the L instances, while the average time of the strategy MSCRP3+VIs* for CS instances was 1,810 seconds. Furthermore, the average gap was smaller in the instances of set L. Moreover, on average, the instances at a higher number of crews were harder to solve.

Table 6: Average results of the MCSRP3+VIs and MCSRP3+VIs* strategies.

Instance	Solution method	#Crew	#Ins	#Opt	%Opt	Avg. upper bound	Avg. lower bound	Avg. gap (%)	Avg. time (seconds)
Set L	MCSRP3 + VIs	1	144	126	87.50	11,251	9,231	5.42	578.49
		3	144	117	81.25	5,562	4,420	5.47	734.53
		5	144	118	81.94	4,734	3,725	6.35	710.60
	MCSRP3 + VIs*	1	144	126	87.50	11,104	9,810	3.68	633.61
		3	144	129	89.58	5,321	4,756	3.11	761.51
		5	144	128	88.89	4,390	3,977	3.54	763.07
Set CS	MCSRP3 + VIs	1	114	85	74.56	127,720	115,219	5.26	1,247.62
		3	114	63	55.26	80,824	64,543	10.78	1,884.45
		5	114	60	52.63	72,640	59,176	13.05	2,024.23
	MCSRP3 + VIs*	1	114	86	75.44	126,348	116,578	4.16	1,396.17
		3	114	84	73.68	73,970	69,258	4.18	1,950.79
		5	114	71	62.28	69,881	63,952	5.79	2,083.51

Finally, Figure 5 presents the percentage of CS instances solved to optimality and the average elapsed times for different values of β. β is the factor by which the distance of a relief path $0-i$

can increase in relation to its shortest distance $dist_{0i}$. Then, $l_i^{\mathsf{d}} = (1+\beta)\cdot dist_{0i}$, and thus larger β values imply larger maximum distances l_i^{d} in the relief paths. As the results indicate, the larger the β's, the easier to solve the corresponding instance. In fact, when the constraints related to the maximum distances are relaxed ($\beta = \infty$), all instances are solved to optimality and the average elapsed time decreases more than 88% in relation to the case with $\beta = 5$. Basically, by allowing larger values for l_i^{d}, it is rather straightforward to find non-dominated relief paths, which increases the effectiveness of the inequalities proposed in Property 1. Also, with larger l_i^{d} values, the non-dominated relief paths tend to use fewer damaged nodes, thus reducing the number of repaired nodes and, consequently, simplifying the crew scheduling and routing decisions. In general, MCSRP3 + VIs* is able to return good-quality solutions within 1 hour of time limit for most of the practical instances, which is a reasonable time considering that the multicrew approach can significantly reduce the accessibility time of the demand nodes, as shown in the next section.

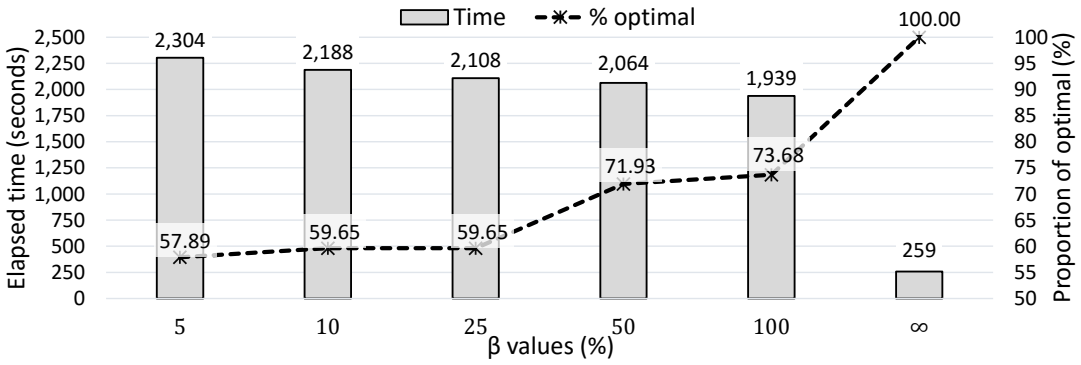

Figure 5: Proportion of optimal instances and average elapsed times for different values of β.

6.3 Practical Relevance: Road restoration in the Megadisaster of Rio de Janeiro in 2011

We now analyze our case study based on the so-called megadisaster of the Serrana Region in Rio de Janeiro, Brazil. This event that occurred in 2011 was characterized by heavy rain, floods, and landslides, compromising water, electricity, and transportation infrastructure systems. It claimed hundreds of lives and affected thousands of people (Rio de Janeiro, 2011). Figure 6 shows the main cities and highways affected by the disaster, according to the Legislative Assembly of Rio de Janeiro (Rio de Janeiro, 2011). Figure 6 reveals that some cities (PE, TE, AR, TR, SA, SU, SJ) can be connected to the depot without using damaged nodes. For these cities, the proposed formulations found the optimal relief paths whose accessibility time was zero. For the other cities (NF, CO, BJ, MA, SS, SM), at least one damaged node have to be used to define the relief paths.

A total of 342 CS instances were derived from the real case disaster by considering different number of damaged nodes, crews, and β values, as described in C. The average results of the CS instances are presented in Table 7. This table shows the total cost; the proportion of nodes repaired (% rep); the proportion of the repaired nodes that are used only in the relief paths (%

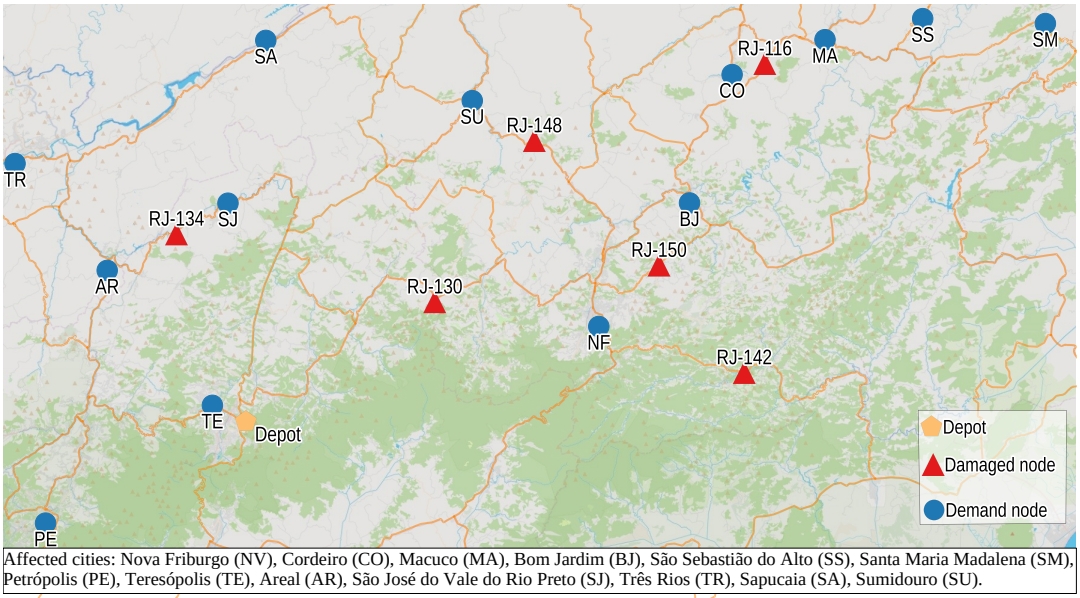

Figure 6: Main cities and highways affected by the disaster.

rep relief paths), i.e., repaired nodes not used in the middle of crew paths; the proportion of required crews (% crew used); the proportion of demand nodes that need at least one damaged node to become accessible (% demand nodes); the best-case, the worst-case and the average accessibility time between demand nodes (best, worst, mean); the total accessibility time of the demand nodes (total); the difference between the worst-case and the best-case accessibility time (range = worst - best); and the average distance of the relief paths in kilometers.

The average proportion of nodes repaired was 42.85%. Thus, not all damaged nodes must be repaired to recover the accessibility of the network. Repaired damaged nodes are used in relief paths and/or crew paths. On average, 87.77% of the repaired damaged nodes were used in the relief paths only. The other repaired nodes were used in both the crew paths and the relief paths. As expected, the problem prioritizes the restoration of the damaged nodes in the relief paths. The proportion of repaired damaged nodes is not significantly affected by the number of crews. In fact, although the average proportion of repaired damaged nodes increases by 2.13% from 42.33 with 1 crew to 43.23 with 5 crews, for some instances the number of repaired damaged nodes decreases. This is the case of instance with $\beta = 5$ in class CS0, represented by the network given in Figure 6 and with optimal schedule shown in Figure 7.

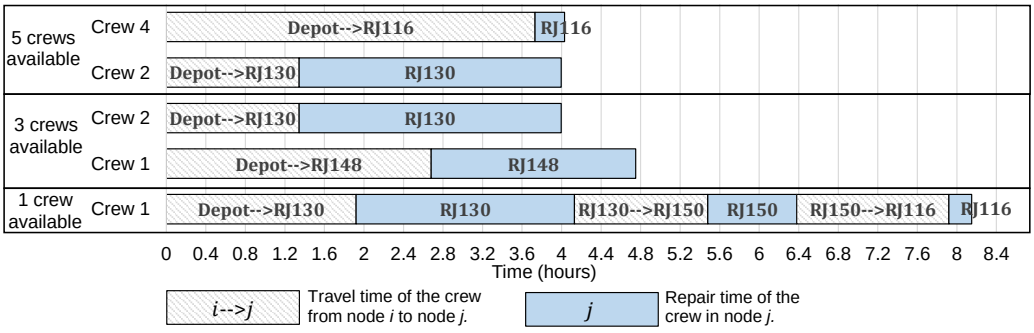

Figure 7: Scheduling of the crews.

Table 7: Average results for different number of crews, damaged nodes, and β values.

Damaged nodes	# crew	β (%)	Total cost	% rep	% rep relief paths[1]	% crew used[1]	% demand nodes	Accessibility time (hours)[2] Best	Worst	Mean	Total	Range	Dist. relief paths (km)
6	1	5	151,737	73.81	91.43	100.00	80.00	2.93	17.23	9.97	136.40	14.30	86.54
		10	150,029	69.05	91.43	100.00	76.70	2.93	16.53	9.86	134.39	13.60	86.67
		25	135,733	64.29	94.29	100.00	72.36	2.87	16.18	7.60	93.95	13.30	91.03
		50	49,487	40.48	88.89	100.00	52.80	2.23	7.20	3.65	37.43	4.97	100.92
		100	44,736	40.48	88.89	100.00	42.36	2.23	7.20	3.26	25.62	4.97	159.87
		∞	0.00	0.00	NA	NA	0.00	0.00	NA	NA	NA	NA	288.31
	3	5	88,574	71.43	90.71	90.48	80.00	1.99	7.40	4.66	61.50	5.41	86.07
		10	88,279	69.05	87.86	85.71	76.70	1.99	7.29	4.63	59.57	5.31	86.49
		25	80,576	66.67	90.00	85.71	72.36	1.92	7.51	4.17	50.24	5.59	90.71
		50	35,647	40.48	94.44	77.78	52.80	1.06	3.47	2.26	24.28	2.41	101.37
		100	33,146	40.48	94.44	77.78	42.36	1.71	3.52	2.25	17.75	1.81	164.84
		∞	0.00	0.00	NA	NA	0.00	0.00	NA	NA	NA	NA	288.31
	5	5	83,994	71.43	90.71	68.57	80.00	1.92	6.24	4.15	53.38	4.32	86.09
		10	83,715	69.05	90.71	62.86	76.70	1.92	6.24	4.15	51.66	4.32	86.47
		25	74,876	66.67	92.86	60.00	72.36	1.92	6.14	3.68	42.90	4.22	90.55
		50	35,413	42.86	83.33	53.33	52.80	1.06	3.47	2.21	23.87	2.41	101.24
		100	32,748	40.48	94.44	53.33	42.36	1.71	3.47	2.23	17.58	1.77	165.63
		∞	0.00	0.00	NA	NA	0.00	0.00	NA	NA	NA	NA	288.31
10	1	5	231,130	63.33	81.49	100.00	89.87	4.51	28.36	15.44	231.52	23.85	87.44
		10	226,349	61.67	81.19	100.00	89.87	4.51	28.40	14.53	217.88	23.89	88.66
		25	207,713	53.33	82.22	100.00	89.87	3.15	24.21	10.84	157.17	21.06	91.54
		50	92,286	38.33	91.67	100.00	67.50	2.77	12.36	6.53	70.65	9.59	104.66
		100	82,477	35.00	87.50	100.00	55.32	2.77	11.15	5.52	46.99	8.38	168.40
		∞	16,058	6.67	100.00	100.00	35.45	1.23	1.23	1.23	7.45	0.00	379.33
	3	5	125,001	63.33	81.09	100.00	89.87	2.06	11.02	6.34	93.67	8.96	87.58
		10	123,009	61.67	80.79	100.00	89.87	2.06	11.02	5.87	87.84	8.96	87.89
		25	113,911	55.00	76.11	100.00	89.87	2.06	9.22	4.99	74.59	7.15	91.50
		50	58,984	41.67	80.00	83.33	67.50	1.95	6.01	3.49	38.90	4.07	104.53
		100	52,608	35.00	84.72	77.78	55.32	1.95	5.70	3.29	27.57	3.75	169.99
		∞	7,152	6.67	100.00	33.33	35.45	0.92	0.92	0.92	3.64	0.00	381.81
	5	5	117,847	63.33	81.09	90.00	89.87	2.02	8.78	5.51	81.02	6.76	87.03
		10	115,892	61.67	86.35	86.67	89.87	2.01	8.80	5.09	75.45	6.79	87.95
		25	105,184	56.67	82.22	83.33	89.87	1.97	7.83	4.33	63.42	5.86	91.28
		50	58,061	41.67	75.83	63.33	67.50	1.92	5.07	3.32	37.16	3.15	104.44
		100	51,917	35.00	70.83	56.67	55.32	1.92	4.55	3.17	26.33	2.63	175.49
		∞	7,152	6.67	100.00	20.00	35.45	0.92	0.92	0.92	3.64	0.00	369.50
14	1	5	259,270	57.14	81.35	100.00	90.71	3.82	34.96	18.81	281.70	31.14	86.91
		10	255,115	55.95	87.37	100.00	90.71	3.82	35.36	17.69	265.60	31.54	88.73
		25	227,120	40.48	83.33	100.00	89.87	3.87	25.34	12.25	173.00	21.47	94.79
		50	87,220	29.76	86.11	100.00	74.68	2.02	12.49	6.12	76.06	10.46	104.62
		100	79,207	27.38	91.67	100.00	64.17	2.02	11.45	5.46	56.55	9.43	144.62
		∞	16,317	4.76	100.00	100.00	35.45	1.24	1.24	1.24	7.55	0.00	417.68
	3	5	152,538	59.52	78.41	100.00	90.71	2.39	13.82	8.12	119.36	11.43	87.09
		10	146,287	57.14	83.50	100.00	90.71	2.60	14.36	7.80	115.61	11.75	88.03
		25	129,439	42.86	86.35	100.00	89.87	1.69	10.92	6.00	87.77	9.23	93.30
		50	57,273	30.95	91.67	88.89	74.68	1.52	6.48	3.81	48.86	4.96	105.80
		100	51,413	27.38	87.50	83.33	64.17	1.52	6.60	3.49	36.96	5.08	149.84
		∞	7,255	4.76	100.00	33.33	35.45	0.92	0.92	0.92	3.68	0.00	393.31
	5	5	137,891	58.33	83.37	90.00	90.71	1.99	12.82	6.95	102.79	10.83	87.11
		10	136,825	55.95	82.90	86.67	90.71	1.99	11.69	6.69	99.29	9.71	87.85
		25	117,443	45.24	83.97	83.33	89.87	1.64	10.71	5.21	75.74	9.06	93.31
		50	56,273	30.95	85.56	63.33	74.68	1.52	5.41	3.59	46.30	3.89	104.35
		100	49,479	27.38	95.83	50.00	64.17	1.52	5.57	3.17	33.62	4.05	146.69
		∞	7,255	4.76	100.00	20.00	35.45	0.92	0.92	0.92	3.68	0.00	434.01
Average per number of crews		1	128,444	42.33	88.75	100.00	66.54	2.88	17.11	8.82	118.82	14.23	148.37
		3	75,061	43.00	87.51	83.38	66.54	1.78	7.42	4.30	55.99	5.64	147.69
		5	70,665	43.23	87.06	64.20	66.54	1.70	6.39	3.84	49.29	4.69	149.29
Average per β (%) values		5	149,776	64.63	84.41	93.23	86.86	2.62	15.63	8.89	129.04	13.00	86.87
		10	147,278	62.35	85.79	91.32	85.76	2.65	15.52	8.48	123.03	12.87	87.64
		25	132,444	54.58	85.71	90.26	84.04	2.34	13.12	6.56	90.98	10.77	92.00
		50	58,961	37.46	86.39	81.11	64.99	1.78	6.88	3.89	44.83	5.10	103.55
		100	53,081	34.29	88.43	77.65	53.95	1.93	6.58	3.54	32.11	4.65	160.60
		∞	6,799	3.81	100.00	51.11	23.63	1.03	1.03	1.03	4.94	0.00	360.06
Average all			91,390	42.85	87.77	82.53	66.54	2.12	10.31	5.65	74.70	8.19	148.45

[1] Values computed considering only the solutions with at least one repaired damaged node.
[2] Values computed considering only the demand nodes with accessibility time higher than 0.
NA: Not available.

Note in Figure 7 that with one crew, three damaged nodes (RJ-130, RJ-116, RJ-150) were repaired to restate the accessibility of the network after 8.15 hours. With three crews, the

total time to restate the accessibility of the network decreased to 4.75 (41.71%) hours. Only two damaged nodes (RJ-130, RJ-148) were repaired in this case. With five crews, the solution indicates the restoration of two damaged nodes (RJ-130, RJ-116), and the time to restate the accessibility of the network was 4.03 hours, a reduction of 15.15% in relation to the case with 3 crews. A trade-off can be observed between increasing the number of crews, which may have a logistic cost in practice, and reducing the time to restore the accessibility of the demand nodes. However, at some point, increasing the number of crews may not significantly affect the accessibility time of the demand nodes. For the instance with $\beta = 5\%$ in class CS0, for example, no significant improvement was observed when five additional crews with the same characteristics than the first five crews were considered. Consequently, when the number of crews increases, more crews can become idle. Note in Table 7 that the utilization of the crews decrease from 100% with one crew to 64.20% with 5 crews.

Insight 1. *There is a remarkable trend in avoiding the damaged nodes not only in the relief paths but also in the route of the crews; thus, only a (usually) small number of damaged nodes end up being repaired to restore the accessibility of the network. Consequently, a further increase in the number of crews is not necessarily followed by a relevant reduction in the accessibility time. In spite of it, if the decision-maker hires more crews, it is likely that some of them will become idle.*

More crews evidently cause a decrease in the accessibility time and, consequently, in the worst-case accessibility time. However, the impact concerning the average accessibility time was less pronounced when we have increasingly more crews, especially in networks with fewer damaged nodes. For example, the average accessibility time with 6 damaged nodes and $\beta = 5\%$ decreased from 9.97 with 1 crew to 4.66 (53.26%) with three crews, while the reduction in the average accessibility time from 3 to 5 crews was 10.94%. Additionally, our results reveal that the multiple crews have a more pronounced effect in reducing the worst-case accessibility time between the demand nodes. For the instances with 6 damaged nodes and $\beta = 5\%$, the reduction in the worst-case accessibility time was 15.68% from three to five crews, while the reduction in the best-case accessibility time was 3.52%. Figure 8 shows the accessibility times of the instance with $\beta = 5\%$ in class CS0 for different numbers of crews. For this particular case, the worst-case accessibility was reduced 50.55%, from 8.15 hours with 1 crew to 4.03 hours with 5 crews.

Insight 2. *Multiple crews help to decrease the accessibility time and to achieve more equitable accessibility times across the different demand nodes, which is a desirable feature in post-disaster settings.*

Figure 8 also illustrates the damaged nodes used in the relief paths to reach the demand nodes. For instance, the relief path to reach MA with one crew is defined by D→RJ-130→BJ→CO→RJ-116→MA. We did not consider intersection nodes in Figure 8. With one crew, MA was the last demand node to become connected, which occurred after 8.15 hours, when nodes RJ-116 and RJ-130 were repaired. SSA became connected after RJ-130 and RJ-150 were repaired while NF, CO, BJ, and SM became connected after RJ-130 was repaired. As expected, the cities with

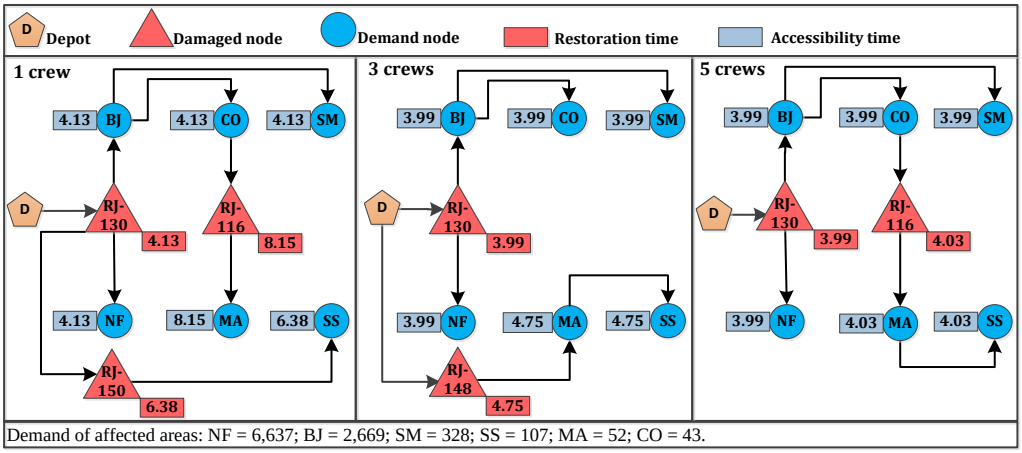

Figure 8: Nodes used in the relief paths to connect the depot with the demand nodes.

greater demand, NF and BJ, were some of the first cities to become accessible after 4.13 hours. However, some cities that have a smaller demand, such as CO and SM, also became accessible within 4.13 hours.

Insight 3. *Cities with greater demand are likely to be the first to become accessible from the depot. However, some cities with smaller demand can also became quickly accessible when their corresponding relief paths use the same damaged nodes as the relief paths associated with the cities with greater demand.*

With three crews, SS and MA became connected after RJ-148 was repaired, while NF, CO, BJ and SM became connected after RJ-130 was repaired. With five crews, SS and MA became connected after RJ-130 and RJ-116 were repaired, while NF, CO, BJ and SM became connected after RJ-130 was repaired. In the cases with 3 and 5 crews, only two crews performed the restoration of two damaged node. However, the repaired damaged nodes changed depending on the characteristics of the crews. For the considered instance, although two crews were enough to perform the restoration, the use of crew 4 instead of crew 1 reduced the total time to restate the accessibility of the network. The relief paths were also affected by the characteristics of the crews. For instance, relief path $0 - SM$ using RJ-116 is a good relief path only when crew 4 is available. Particularly, damaged node RJ-116 has a short repair time but it is far away from the depot. Crew 4, that has shorter travel times than crew 1, can perform a faster restoration of RJ-116. Consequently, RJ-116 became better than RJ-150 (used in the case with one crew) and RJ-148 (used in the case with three crews) in the relief path $0 - SM$. In general, when multiple crews are available, farther damaged nodes are usually allocated to the crews with shorter travel times to those nodes, while damaged nodes with longer repair times are allocated to crews that can perform a faster restoration, thus saving travel and restoration times, respectively. Moreover, the crews are usually allocated to repair groups of damaged nodes that are geographically close to each other, which also saves time.

Insight 4. *The heterogeneous characteristics of the crews can significantly affect the scheduling and relief paths decisions of the problem. The allocation of the crews to the damaged nodes depends on their characteristics, location of the damaged nodes, and repair times.*

Interestingly, in Figure 8 we can observe that SS and SM required repairing different damaged nodes to be accessible, even though such cities are geographically close to one another. The reason for this result is the maximum distance $l_i^{\mathtt{d}}$ allowed for the relief paths. For SS and SM, the maximum distances were $l_{SS}^{\mathtt{d}} = 156.27$ and $l_{SM}^{\mathtt{d}} = 165.41$, respectively. The feasible relief paths $0 - SS$ used one of the damaged nodes RJ-150, RJ-148 or RJ-116, while there was a relief path $0 - SM$ that did not require the use of those nodes. Such an alternative path was shorter than $l_{SM}^{\mathtt{d}}$ and then feasible to reach SM, but it was higher than $l_{SS}^{\mathtt{d}}$ and then infeasible to reach SS. If $l_{SS}^{\mathtt{d}}$ increases to 165, it would be possible to define a path to SS without using any of damaged nodes RJ-150, RJ-148 or RJ-116.

Insight 5. *The definition of the path to reach the demand nodes from the depot is not trivial since even nodes that can be geographically near each other could require the restoration of different nodes to become accessible. The reason for such behavior is mainly the maximum distance $l_i^{\mathtt{d}}$ imposed for the relief paths. The decision-maker should select $l_i^{\mathtt{d}}$ carefully since even small changes in this parameter for a given demand node i might lead to significantly different solutions.*

Table 7 reveals that the maximum distance $l_i^{\mathtt{d}}$, which is computed using different β values, can significantly affect the accessibility time and the number of repaired damaged nodes in the problem. Evidently, the accessibility time decreases for larger β values, mainly because more feasible relief paths are available. A straightforward consequence of having more feasible relief paths is the reduced number of demand nodes that need the restoration of at least one damaged node to be accessible since the additional relief paths might not require the use of such damaged nodes. For instance, the average number of demand nodes that require damaged nodes to become accessible decreases from 86.86% with $\beta = 5$ to 23.63% with $\beta = \infty$. In contrast, the average distance of the relief paths increases significantly for larger choices of β. Note, e.g., that the average distance increases more than four times, from 86.87 km when $\beta = 5\%$ to 360.06 km when $\beta = \infty$. Larger values of β imply in the restoration of fewer damaged nodes. In fact, when the maximum distance constraint is relaxed, no damaged node need to be repaired to recover the accessibility of the network in some cases. For example, damaged networks with 6 damaged nodes and $\beta = \infty$ did not require the restoration of these nodes. A clear example of this situation is the instances in class CS0 defined by the network in Figure 6, in which it is possible to find relief paths without requiring damaged nodes if $\beta = \infty$. However, when the number of damaged nodes increases, they become necessary to define the relief paths, even in the cases with $\beta = \infty$.

Insight 6. *In general, shorter maximum distances imply fewer feasible relief paths, which may increase the accessibility time of the demand nodes and increase the number of repaired damaged nodes. Longer maximum distances may reduce the accessibility time of the demand nodes and the number of repaired damaged nodes. However, they can lead to the selection of longer relief paths, which is undesirable in practical distribution or evacuation operations in post-disaster situations. Evidently, there is a trade-off between good accessibility times and the quality of the relief paths in terms of distance.*

Finally, Figure 9 illustrates the average accessibility time for different number of damaged nodes and instance classes. On average, the increase in the damaged nodes in a network of

a given class increases the accessibility time of the solutions. However, such behavior can be different when we compare instances of different classes. For example, the average accessibility time for the instances of class CS4 with 10 damaged nodes was 6.76, while for the instances of class CS6 with 14 damaged nodes was 5.85 (13.46% smaller). Therefore, the increase in the accessibility time depends not only on the number of damaged nodes but also on the location of the damaged nodes. In Figure 6, for example, it is possible to observe some regions where fewer damaged nodes disrupting the accessibility could have a higher impact than a higher number of damaged nodes in regions where there is no demand nodes.

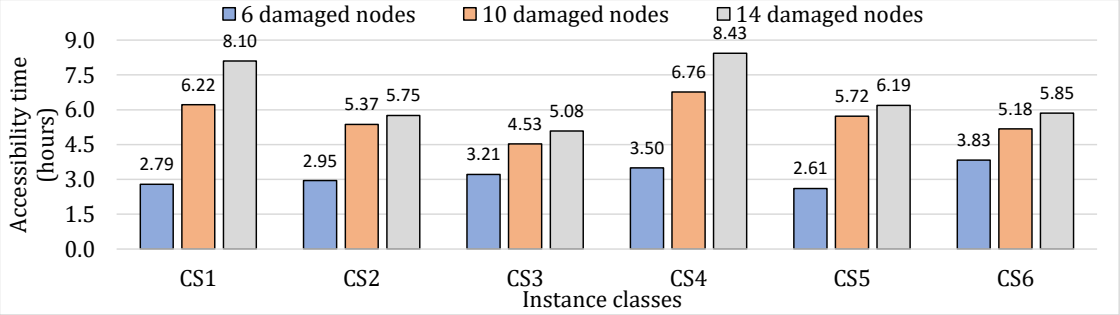

Figure 9: Average accessibility time for different damaged nodes and instance classes.

7 Conclusions

This paper proposed three novel mathematical formulations for the multicrew scheduling and routing problem in road restoration. New valid inequalities were also developed. The first two formulations are based on the three-index and two-index formulation of the VRP. The third formulation eliminates a few variables and introduces new constraints to reduce the symmetry in the solutions of the problem. The valid inequalities are based on the dominance of the paths between nodes in the damaged network. We performed computational experiments using instances from the literature and based on a real disaster situation. The three mathematical formulations showed improvement with the addition of the VIs. The model based on the two-index VRP formulation showed the best performance for most of the instances. Furthermore, the elimination of symmetric solutions in the third formulation improved the performance of the model, especially in finding feasible solutions. The model based on the three-index VRP formulation provides optimality guarantees for a higher number of instances, but it has difficulty finding feasible solutions in some cases. The graph reduction strategy for deriving cuts from networks with fewer nodes also improves the results. Thus, the best approach was able to obtain good-quality solutions with less than 7% of the average optimality gap for the different instance classes.

The analysis of the practical case showed that, as expected, the use of more crews to solve the problem significantly reduces the time required to make the demand nodes accessible. However, the impact concerning the average accessibility time was less pronounced when we had increasingly more crews, especially in the networks with fewer damaged nodes. The multiple crews mainly affect the worst-case accessibility time between the demand nodes, thus providing

more equitable accessibility times. Usually, the farthest damaged nodes were allocated to the crews that had the shortest travel time, while the damaged nodes with higher repair time were allocated to crews that can perform a faster restoration. The restoration of damaged nodes in the relief paths was prioritized over nodes in the crew paths. A few additional damaged nodes are repaired only if they are strictly necessary in the path of the crews to reach other damaged nodes. Furthermore, on average, fewer than 55% of the damaged nodes were required to restore the accessibility of the network. Such a proportion decreased when paths with higher distances were allowed to connect the depot with the demand nodes, but it is not significantly affected by the increase in the number of available crews.

We believe that the current research could be further developed in a number of directions. First, as repair and/or travel times can be difficult to estimate in the immediate disaster aftermath, alternative formulations to handle uncertainty settings should be investigated. Second, modeling the interaction or synergy of more than one crew could help to further reduce accessibility times, thus this is also a promising future development. Finally, it would be useful to strengthen our collaboration with humanitarian organizations to get feedback from practitioners on the usefulness of our mathematical models and algorithms. Certainly, we would need to build a user-friendly tool first to show the solutions we can come up with. Such feedback would be fundamental to refine the models and better understand the relevance of our approach.

Acknowledgements

This work was supported by the São Paulo Research Foundation (FAPESP) [grant numbers 2015/26453-7, 2016/15966-6 and 2016/23366-9]; and the National Council for Scientific and Technological Development (CNPq) [grant numbers 141973/2016-1 and 304601/2017-9]. The second author thanks the support of both the British Academy via BA/Leverhulme Small Research Grant SRG18R1\180939 and the UEBS First Grant Venture Fund. The operation of the server mp2b used to run the computational experiments is funded by the Canada Foundation for Innovation (CFI), the ministère de l'Économie, de la science et de l'innovation du Québec (MESI) and the Fonds de recherche du Québec - Nature et technologies (FRQ-NT).

A NP-hardness proof of the MCSRP

Proposition 5. *The MCSRP is NP-hard.*

Proof. To prove that the MCSRP is NP-hard, we prove that the MCSRP is at least as hard as the traveling salesman problem (TSP). For this purpose, let us consider a TSP problem over a complete graph $G = (N, E)$, with $N = \{0, 1, 2, \ldots, n\}$. Node 0 represents the origin city. Let c_{ij} be the travel cost from node i to node j. We assume that the travel costs satisfy the triangular inequality. The TSP can be easily reduced to a MCSRP instance, as presented in Figure 10, under the following assumptions:

- Only one crew is available.
- Node 0 represents the depot.
- A dummy node n' is introduced in the same position of the depot, but representing a damaged node. There is not arc connecting node 0 to node n'.
- There is only one demand node f and it is connected solely to node n'.
- The demand of node f is $d_f = 1$ and the maximum distance allowed for relief path $0 - f$ is $l_f^d = |N| + 1$.
- The repair time is null ($\delta_{kj} = 0$) and the shortest travel time of crew k between nodes i and j without using damaged nodes is

$$\rho_{kij} = \begin{cases} c_{ij}, & \text{if } i \in N \text{ and } j \in N, \\ c_{i0}, & \text{if } i \in N \setminus \{0\} \text{ and } j = n', \\ M, & \text{otherwise}, \end{cases} \tag{80}$$

  where M is large enough. Since we assume that the TSP instance satisfies triangular inequality, the shortest path from node i to node j is the direct arc e connecting nodes $i - j$. The travel time τ_{ke} of crew k on arc e connecting nodes i and j is set as ρ_{kij}.

- The length of arcs $e \in E$ is

$$\ell_e = \begin{cases} 1, & \text{if arc } e \text{ connects nodes } i - j, \text{ for } i \in N, j \in N \text{ and } j = i + 1, \\ 1, & \text{if arc } e \text{ connects nodes } n - n' \text{ or } n' - f, \\ M, & \text{otherwise}, \end{cases} \tag{81}$$

  where M is large enough. This way, given that $l_f^d = |N| + 1$, the only feasible relief path is $0 \to 1 \to 2 \to \ldots \to n \to n' \to f$. Consequently, the optimal relief path $0 - f$ uses all the damaged nodes and all the damaged nodes should be repaired. The relief path $0 - f$ does not define the sequence of the restoration, which is defined by the scheduling decisions.

The optimal objective function value of the MCSRP instance is

$$d_f \cdot Z_f^{\mathrm{d}} = d_f \cdot \max_{j \in N \cup \{n'\}} \{Z_j^{\mathrm{r}}\}.$$

Given that $\rho_{kn'j} = M,\ \forall j \in N$, n' should be the last damaged node repaired by the crew in the optimal solution of the MCSRP. Then,

$$\max_{j \in N \cup \{n'\}} \{Z^{\mathtt{r}}_j\} = Z^{\mathtt{r}}_{n'} = \sum_{i \in N} \sum_{j \in N \cup \{n'\}} (\delta_{kj} + \rho_{kij}) \hat{X}_{kij} = \sum_{i \in N} \sum_{j \in N \cup \{n'\}} c_{ij} \hat{X}_{kij},$$

where $\hat{X}_{kij}$ indicates if node j was repaired immediately after node i. Therefore,

$$d_f \cdot Z^{\mathtt{d}}_f = \sum_{i \in N} \sum_{j \in N \cup \{n'\}} c_{ij} \hat{X}_{kij},$$

which is the same cost of this solution in the TSP instance. Thus, by solving the MCSRP instance presented in Figure 10, we can obtain a solution with the same objective value for the TSP problem. Since the TSP is known to be an NP-hard problem, the MCSRP must be also NP-hard. □

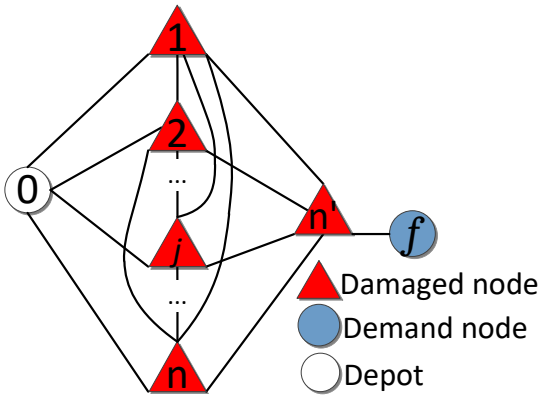

Figure 10: MCSRP instance created from the TSP instance.

Note that we proof the NP-hardness of the MCSRP by considering the particular case when one crew is available. Consequently, we also prove that the SCSRP is NP-hard.

B VIs related to routing decisions for the second and third MCSRP formulations

Inequalities (82)-(85) are the valid inequalities related to routing decisions for MCSRP2. Inequalities (82),(83) are equivalent to inequalities (75),(76) to select non-dominated paths over dominated paths. Inequalities (84), (85) are equivalent to inequalities (78), (79) to set lower bounds for the variables $Z^{\mathtt{r}}_j$.

$$\begin{aligned}
&\sum_{e \in E_{f^*_{kij}}} P_{eij} + \sum_{l \in \mathcal{V}^{\mathtt{u}}_{f^*_{kij}}} N^{\mathtt{u}}_{lij} \geq (|E_{f^*_{kij}}| + |\mathcal{V}^{\mathtt{u}}_{f^*_{kij}}|) \cdot (X'_{ij} + W'_{kj} - 1), \\
&\forall k \in \mathcal{K}, i \in \mathcal{V}^{\mathtt{r}}_0, j \in \mathcal{V}^{\mathtt{r}} : \mathcal{F}^{\mathtt{r}*}_{kij} \neq \emptyset, t_{kf^*_{kij}} = t_{kp^*_{kij}}, \qquad (82) \\
&(|E| + |\mathcal{V}|) \cdot (2 + |\mathcal{V}^{\mathtt{r}}_p| - X'_{ij} - W'_{kj} - \sum_{h \in \mathcal{R}} \sum_{l \in \mathcal{V}^{\mathtt{r}}_p} N^{\mathtt{r}}_{lhij}) \geq \sum_{e \in E \setminus \bigcup_{p' \in \mathcal{D}_p} E_{p'}} P_{eij} + \sum_{l \in \mathcal{V} \setminus \bigcup_{p' \in \mathcal{D}_p} \mathcal{V}_{p'}} N^{\mathtt{u}}_{lij},
\end{aligned}$$

$$\forall\ k \in \mathcal{K},\ i \in \mathcal{V}_0^{\mathrm{r}},\ j \in \mathcal{V}^{\mathrm{r}}, p \in \mathcal{S}_{kij}^{\mathrm{r}} : (\mathcal{F}_{kij}^{\mathrm{r}*} = \emptyset) \vee (\mathcal{F}_{k0j}^{\mathrm{r}*} \neq \emptyset, p \neq f_{kij}^*, t_{kf_{kij}^*} > t_{kp_{kij}^*}), \tag{83}$$

$$Z_j^{\mathrm{r}} \geq (t_{kp_{k0j}^*} + \delta_{kj}) \cdot X'_{0j} + \sum_{i \in \mathcal{V}^{\mathrm{r}}} ((t_{kp_{k0i}^*} + \delta_{ki} + t_{kp_{kij}^*} + \delta_{kj}) \cdot X'_{ij}) - M \cdot (1 - W'_{kj}),$$

$$\forall\, k \in \mathcal{K},\ j \in \mathcal{V}^{\mathrm{r}}, \tag{84}$$

$$Z_j^{\mathrm{r}} \geq Z_i^{\mathrm{r}} + t_{kp_{kij}^*} + \delta_{kj} - M \cdot (2 - W'_{kj} - X'_{ij}), \forall\, k \in \mathcal{K},\ i \in \mathcal{V}_0^{\mathrm{r}},\ j \in \mathcal{V}^{\mathrm{r}}. \tag{85}$$

Inequalities (84),(85) are the same for MCSRP3. Additionally, we can state the following valid inequalities for this formulation.

$$\sum_{e \in E_{f_{k0j}^*}} P_{e0j} + \sum_{l \in \mathcal{V}^{\mathrm{u}}_{f_{k0j}^*}} N^{\mathrm{u}}_{l0j} \geq (|E_{f_{k0j}^*}| + |\mathcal{V}^{\mathrm{u}}_{f_{k0j}^*}|) \cdot (X'_{0j} + W'_{kj} - 1),$$

$$\forall k \in \mathcal{K}, j \in \mathcal{V}^{\mathrm{r}} : (\mathcal{F}_{k0j}^{\mathrm{r}*} \neq \emptyset, t_{kf_{k0j}^*} = t_{kp_{k0j}^*}), \tag{86}$$

$$(|E| + |\mathcal{V}|) \cdot (2 + |\mathcal{V}_p^{\mathrm{r}}| - X'_{0j} - W'_{kj} - \sum_{h \in \mathcal{R}} \sum_{l \in \mathcal{V}_p^{\mathrm{r}}} N^{\mathrm{r}}_{lh0j}) \geq \sum_{e \in E \setminus \bigcup_{p' \in \mathcal{D}_p} E_{p'}} P_{e0j} + \sum_{l \in \mathcal{V} \setminus \bigcup_{p' \in \mathcal{D}_p} \mathcal{V}_{p'}} N^{\mathrm{u}}_{l0j},$$

$$\forall\ k \in \mathcal{K},\ j \in \mathcal{V}^{\mathrm{r}}, p \in \mathcal{S}_{k0j}^{\mathrm{r}} : (\mathcal{F}_{k0j}^{\mathrm{r}*} = \emptyset) \vee (\mathcal{F}_{k0j}^{\mathrm{r}*} \neq \emptyset, p \neq f_{k0j}^*, t_{kf_{k0j}^*} > t_{kp_{k0j}^*}) \tag{87}$$

$$\sum_{e \in E_{f_{kij}^*}} P_{eij} + \sum_{l \in \mathcal{V}^{\mathrm{u}}_{f_{kij}^*}} N^{\mathrm{u}}_{lij} \geq (|E_{f_{kij}^*}| + |\mathcal{V}^{\mathrm{u}}_{f_{kij}^*}|) \cdot (X'_{ij} + X'_{ji} + W'_{kj} - 1),$$

$$\forall k \in \mathcal{K}, i \in \mathcal{V}^{\mathrm{r}}, j \in \mathcal{V}^{\mathrm{r}} : (\mathcal{F}_{kij}^{\mathrm{r}*} \neq \emptyset, t_{kf_{kij}^*} = t_{kp_{kij}^*}, i < j), \tag{88}$$

$$(|E| + |\mathcal{V}|) \cdot (2 + |\mathcal{V}_p^{\mathrm{r}}| - X'_{ij} - X'_{ji} - W'_{kj} - \sum_{h \in \mathcal{R}} \sum_{l \in \mathcal{V}_p^{\mathrm{r}}} N^{\mathrm{r}}_{lhij}) \geq \sum_{e \in E \setminus \bigcup_{p' \in \mathcal{D}_p} E_{p'}} P_{eij} + \sum_{l \in \mathcal{V} \setminus \bigcup_{p' \in \mathcal{D}_p} \mathcal{V}_{p'}} N^{\mathrm{u}}_{lij},$$

$$\forall\ k \in \mathcal{K},\ i \in \mathcal{V}^{\mathrm{r}},\ j \in \mathcal{V}^{\mathrm{r}}, p \in \mathcal{S}_{kij}^{\mathrm{r}} : (\mathcal{F}_{kij}^{\mathrm{r}*} = \emptyset, i < j) \vee (\mathcal{F}_{kij}^{\mathrm{r}*} \neq \emptyset, p \neq f_{kij}^*, t_{kf_{kij}^*} > t_{kp_{kij}^*}, i < j). \tag{89}$$

Inequalities (86)-(87) are defined for $i = 0$ and are equivalent to inequalities (82)-(83). Inequalities (88)-(89) are defined for $i \neq 0$ and are equivalent to inequalities (82)-(83).

C Instance generation from the real case disaster

The Megadisaster of the Serrana region of Rio de Janeiro affected different cities and caused traffic blockages due to landslides and flooding in different points of six of the main highways (Rio de Janeiro, 2011). Initially, we have assumed one damaged node in each of the affected highways. Since some of the highways were affected in more than one location, we also generate instances considering a higher number of damaged nodes. The demand in the different cities is shown in Table 8. For cities 1-13 the demand is equal to the number of affected people in the disaster in 2011. There was no reported demand for cities 14-20. Thus, we generate the demand of the cities 14-20 as a proportion of their total population.

The damaged network based on the real disaster is shown in Figure 11. The real distance of the arcs was calculated via Google Maps®. The travel time for a single crew was computed based on the distance and assuming a speed of 25 kilometers per hour for the crew. We have not found information about the repair time of the damaged nodes. This way, for a single crew, we have generated the repair time based on the travel time (which is proportional to the distance) on the highway where the damaged node is located. The idea was to generate higher repair times for longer highways, in general higher than the travel times. Thus, for a single crew, the repair

Table 8: Demand of the affected cities (Rio de Janeiro, 2011).

	City	Demand
1	Nova Friburgo	6,637
2	Cordeiro	43
3	Macuco	52
4	Bom Jardim	2,669
5	São Sebastião do alto	107
6	Santa Maria Madalena	328
7	Petrópolis	7,214
8	São José do Vale do Rio Preto	395
9	Três Rios	9
10	Areal	737
11	Sapucaia	40
12	Teresópolis	17,029
13	Sumidouro	801
14	Conceição de Macabu	782
15	Casimiro de Abreu	1305
16	Trajano de Moraes	454
17	Cachoeiras de Macacu	2005
18	Duas Barras	406
19	Cantagalo	731
20	Carmo	643
Total		42,387

time of a damaged node i located in a given arc (highway) e was randomly generated from the interval $[2 \cdot \text{time}_e\,, 5 \cdot \text{time}_e]$, in which time_e is the travel time on arc e. Travel and repair times for the multiple crews were generated from the values of a single crew, as described in Section 6.1. The maximum distance from the depot to the demand nodes (l_i^{d}) was calculated as in the literature (Maya-Duque et al., 2016; Moreno et al., 2019), using a parameter β that indicates the factor by which the distance between the depot and the demand nodes can increase with respect to the shortest distance. Thus, $l_i^{\mathsf{d}} = (1+\beta) \cdot dist_{0i}$, in which $dist_{0i}$ is the shortest distance between the depot and the demand node i. We consider six values for β (0.05, 0.1, 0.25, 0.5, 1, ∞), where ∞ represents a sufficiently large number indicating that the constraint imposing the maximum distance l_i^{d} is relaxed.

From the damaged network of Figure 11, we generate seven classes of instances. The class CS0 has 6 damaged nodes located in the highways originally affected by the disaster in 2011. Furthermore, class CS0 considers the first 13 cities (cities 1-13) as the demand nodes. Considering the six values for β, a total of 6 instances were generated in class CS0. In class CS1, we have generated 3 damaged networks considering 6, 10 and 14 damaged nodes. Damaged networks in a same class share some damaged nodes. Let CS1-$|\mathcal{V}^r|$ be the damaged network of class CS1 with $|\mathcal{V}^r|$ damaged nodes. In the damaged network CS1-6, the 6 damaged nodes were located in 6 randomly selected arcs. Similar to the categorization used in Akbari and Salman (2017b), we divide the arcs into three groups according to their proximity to the affected areas, as high, medium and low-risk arcs. Then, for the location of a given damaged node, the probability of selecting a high, medium and low-risk arc was set to 0.15, 0.35, and 0.5, respectively. The damaged network CS1-10 considers the 6 damaged nodes in CS1-6 and 4 additional randomly located damaged nodes. Similarly, the damaged network CS1-14 considers the 10 damaged nodes in CS1-10 and 4 additional randomly located damaged nodes. For each one of the three damaged networks, the six values of β were considered, totaling 18 instances in class CS1. The same procedure was used to generate classes CS2 and CS3. Classes CS1-CS3 consider the first

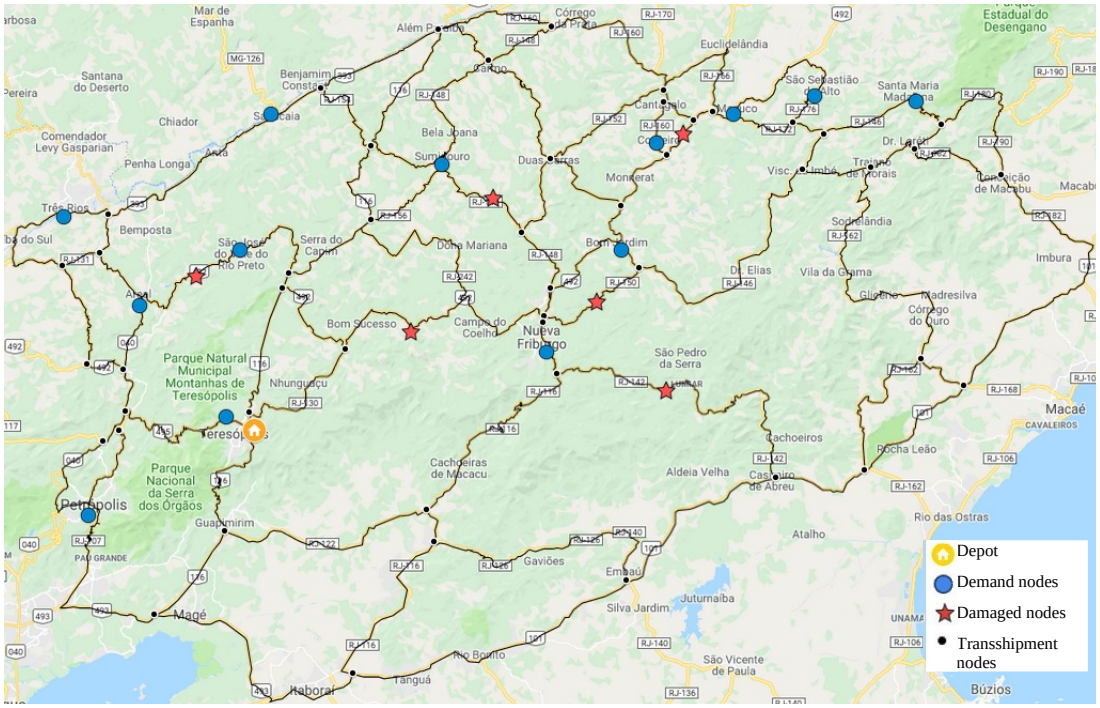

Figure 11: Damaged network based on the real disaster.

13 cities in Table 8 as the demand nodes. Finally, classes CS4-CS6 are based on the the same damaged networks of classes CS1-CS3, but considering all the cities presented in Table 8 as the demand nodes. Thus, there are 114 instances based on the real-world case. We run experiments with 1, 3 and 5 crews, totaling 342 CS instances.

D Graph reduction strategy

Originally proposed by Moreno et al. (2019), the idea of the graph reduction strategy is to set lower bounds for the accessibility time of the affected areas based on the solution of the problem in graphs with a reduced number of demand and damaged nodes. Let $L \subseteq \mathcal{V}^{\mathrm{r}}$ be a subset of the damaged nodes and $F \subseteq \mathcal{V}^{\mathrm{d}}$ be a subset of the demand nodes in the original graph G. G^{LF} is defined as the subgraph obtained from G by deleting all the damaged nodes that are not in L and transforming all the demand nodes that do not belong to F into intersection nodes. The subgraph G^{LF} is further reduced by removing intersection nodes that are not directly connected to damaged nodes. For each node i removed from G^{LF}, the arcs adjacent to this node are deleted and new arcs are created connecting each pair of nodes j and k that were neighbors of i in G^{LF}, such that $j \neq k$. The cost c_{jk} of the new arc $j-k$ is set as $c_{jk} = c_{ji} + c_{ik}$. The resulting graph is denoted by $\bar{G}^{LF}$. From a feasible solution of the MCSRP defined using $\bar{G}^{LF}$, valid inequalities can be derived for the original problem, as pointed out in Proposition 6.

Proposition 6. *Given $L \subseteq \mathcal{V}^{r}$ and $F \subseteq \mathcal{V}^{d}$, let $K^{\bar{G}^{LF}}$ be an optimal solution of the MCSRP defined using the reduced graph $\bar{G}^{LF}$ of the original graph G. Let $\widehat{\Theta}^{\bar{G}^{LF}}$ be the optimal value and $\widehat{\theta}_i^{\bar{G}^{LF}}$ be the value of the variable Z_i^d in the optimal solution $K^{\bar{G}^{LF}}$, for all $i \in F$. Then, the*

following inequalities are valid for the original MCSRP defined using the graph G:

$$\sum_{i \in F:\, d_i \cdot \widehat{\theta}_i^{\bar{G}^{LF}} > 0} d_i \cdot Z_i^d \geq \widehat{\Theta}^{\bar{G}^{LF}}, \tag{90}$$

$$\sum_{j \in L} V_{ji} \geq 1, \forall i \in F : \widehat{\theta}_i^{\bar{G}^{LF}} > 0. \tag{91}$$

Proof. The proof of equation (90) is given in Moreno et al. (2019). If $\widehat{\theta}_i^{\bar{G}^{LF}} > 0$, the relief paths to demand node i use at least one of the damaged nodes in set L, thus equation (91) is valid. □

E Separation algorithms

In this section, we show the separation algorithms developed to obtain sets $\mathcal{P}_i^{\mathtt{d}*}, \mathcal{F}_{kij}^{\mathtt{r}*}, \mathcal{P}_{kij}^{\mathtt{r}*}$, and n_i, which are all based on the shortest path problem (SPP). Algorithm 2 outlines the procedure used to find set $\mathcal{P}_{kij}^{\mathtt{r}*}$. For each i, j, k, the set $\mathcal{P}_{kij}^{\mathtt{r}*}$ is found by solving the SPP between damaged nodes i and j over the original graph $G = (\mathcal{V}, E)$ (line 2 of Algorithm 2) considering the cost τ_{ke} in the arcs $e \in E$ of the graph (line 1 of Algorithm 2) .

Algorithm 2 Algorithm to find set $\mathcal{P}_{kij}^{\mathtt{r}*}$.

`Input:`
Graph $G = (\mathcal{V}, E)$; Indices i, j, k; Parameter τ_{ke}, $\forall e \in E$;
`Output:`
Paths $p \in \mathcal{P}_{kij}^{\mathtt{r}*}$;

1: Set cost τ_{ke}, $\forall e \in E$;
2: Find the shortest path p from node i to node j for crew k over graph G;
3: Insert path p into set $\mathcal{P}_{kij}^{\mathtt{r}*}$;
4: return set $\mathcal{P}_{kij}^{\mathtt{r}*}$;

Algorithm 3 outlines the procedure to find set $\mathcal{F}_{kij}^{\mathtt{r}*}$. Basically, $\mathcal{F}_{kij}^{\mathtt{r}*}$ is found by solving the SPP between damaged nodes i and j over a graph G' (line 8 of Algorithm 3), in which the damaged nodes $l \in \mathcal{V}^r : l \neq i, l \neq j$ and the arcs incident to them are removed (line 5 of Algorithm 3). In this case, the cost of the arcs in G are set as τ_{ke} (line 1 of Algorithm 3). Similarly, Algorithm 4 shows that set $\mathcal{P}_i^{\mathtt{d}*}$ is determined by solving the SPP between the depot and demand node i over the same graph G' (line 8 of Algorithm 4) considering the cost ℓ_e in the arcs $e \in E$ of the graph (line 1 of Algorithm 4).

Algorithm 3 Algorithm to find set $\mathcal{F}^{\mathtt{r}*}_{kij}$.

`Input:`
Graph $G = (\mathcal{V}, E)$; Indices i, j, k; Parameter τ_{ke}, $\forall e \in E$;
`Output:`
Paths $p \in \mathcal{P}^{\mathtt{r}*}_{kij}$;

1: Set cost τ_{ke}, $\forall e \in E$;
2: Set $G' := G$;
3: **for** $l = 1$ **to** $|\mathcal{V}|$ **do**
4: **if** $\{l \in \mathcal{V}^{\mathtt{r}}$ **and** $l \neq i$ **and** $l \neq j\}$ **then**
5: Remove node l and arcs $e \in E_l$ from graph G';
6: **end if**
7: **end for**
8: Find the shortest path p from node i to node j for crew k over graph G';
9: Insert path p into set $\mathcal{F}^{\mathtt{r}*}_{kij}$;
10: return set $\mathcal{F}^{\mathtt{r}*}_{kij}$;

Algorithm 4 Algorithm to find set $\mathcal{P}^{\mathtt{d}*}_{i}$.

`Input:`
Graph $G = (\mathcal{V}, E)$; Index i; Parameter ℓ_e, $\forall e \in E$;
`Output:`
Paths $p \in \mathcal{P}^{\mathtt{d}*}_{i}$;

1: Set cost ℓ_e, $\forall e \in E$;
2: Set $G' := G$;
3: **for** $l = 1$ **to** $|\mathcal{V}|$ **do**
4: **if** $l \in \mathcal{V}^{\mathtt{r}}$ **then**
5: Remove node l and arcs $e \in E_l$ from graph G';
6: **end if**
7: **end for**
8: Find the shortest path p from node 0 to node i over graph G';
9: Insert path p into $\mathcal{P}^{\mathtt{d}*}_{i}$;
10: return set $\mathcal{P}^{\mathtt{d}*}_{i}$;

Finally, set n_i can be determined by solving one SPP for each damaged node $l \in \mathcal{V}^r$. Basically, to know if a damaged node l is an element of n_i, we create a graph G' removing node l and its incident arcs from graph G (line 5 of Algorithm 5), and the SPP between the depot and demand node i is solved (line 6 of Algorithm 5). If there is a path from the depot to demand node i with a cost less than or equal to $l^{\mathtt{d}}_i$, node l is not an element of n_i. Otherwise, we insert node l into n_i (lines 10 and 13 of Algorithm 5).

Algorithm 5 Algorithm to find set n_i.

`Input:`
Graph $G = (\mathcal{V}, E)$; Index i; Parameters ℓ_e, $\forall e \in E$, $l_i^{\mathtt{d}}, \forall i \in \mathcal{V}^{\mathtt{d}}$;
`Output:`
Set n_i;

Set cost ℓ_e, $\forall e \in E$;
for $l = 1$ **to** $|\mathcal{V}|$ **do**
  if $\{l \in \mathcal{V}^{\mathtt{r}}\}$ **then**
    Set $G' := G$;
    Remove node l and arcs $e \in E_l$ from graph G';
    Find the shortest path p from node 0 to node i over graph G';
    if path p exists **then**
      $t_p := \sum_{e \in E_p} \ell_e$;
      if $t_p > l_i^{\mathtt{d}}$ **then**
        Insert node l into n_i;
      end if
    else
      Insert node l into n_i;
    end if
  end if
end for
return set n_i;

F Additional computational results

Tables 9 and 10 show the average results of the three proposed formulations with and without the valid inequalities for different numbers of crews. The average upper bound, lower bound, and gap presented in columns 9 to 11 are computed using all the instances with feasible solutions and hence they cannot be compared directly for different approaches since some of them do not return feasible solutions for some instances. On the other hand, the average upper bound, lower bound and gap presented in columns 6 to 8 are computed using only the results of instances for which all solution approaches found feasible solutions and hence they can be directly compared. These values confirm the discussion presented in Section 6.2, showing that the VIs help to improve the average gap, upper bound and lower bound of the solutions.

Tables 11 and 12 show the average results of the MCSRP3+VIs and MCSRP3+VIs* strategies, respectively, for the different classes of instances.

Table 9: Average results of the three MCSRP models with and without the VIs for the instances from the literature.

Solution method	# Crew	%Feas	%Opt	Avg. time (seconds)	Common feasible instances[1] Avg. upper bound	Common feasible instances[1] Avg. lower bound	Common feasible instances[1] Avg. gap (%)	All feasible instances[2] Avg. upper bound	All feasible instances[2] Avg. lower bound	All feasible instances[2] Avg. gap (%)
MCSRP1	1	84.72	75.00	994.15	8,510	7,103	3.21	9,091	7,119	4.31
	3	84.03	72.22	1,088.66	3,976	3,244	4.07	3,976	3,244	4.07
	5	84.72	72.22	1,113.14	4,000	2,903	4.86	3,950	2,872	4.78
MCSRP2	1	88.89	76.39	926.83	8,456	7,905	1.16	10,098	8,026	3.82
	3	87.50	65.28	1,275.78	3,953	3,194	3.83	4,387	3,304	5.48
	5	86.81	66.67	1,310.07	3,702	2,896	4.76	3,935	2,884	6.49
MCSRP3	1	88.89	77.08	952.37	8,609	7,263	2.45	10,447	7,291	5.33
	3	87.50	68.06	1,208.17	4,055	2,904	6.12	4,352	3,015	7.04
	5	88.19	66.67	1,293.73	3,920	2,796	5.88	4,129	2,752	8.28
MCSRP1 + VIs	1	100.00	86.11	512.33	8,456	8,455	0.00	11,168	9,164	5.61
	3	97.92	86.11	552.49	3,924	3,750	0.75	5,039	4,296	3.76
	5	97.92	88.89	473.48	3,597	3,596	0.00	4,187	3,754	3.45
MCSRP2 + VIs	1	100.00	87.50	466.59	8,456	8,456	0.00	11,675	9,209	5.64
	3	100.00	86.81	574.45	3,923	3,913	0.05	6,615	4,489	5.87
	5	100.00	84.72	669.77	3,598	3,552	0.34	4,616	3,891	5.30
MCSRP3 + VIs	1	100.00	87.50	578.49	8,456	8,453	0.01	11,251	9,231	5.42
	3	100.00	81.25	734.53	3,930	3,811	0.50	5,562	4,420	5.47
	5	100.00	81.94	710.60	3,626	3,464	0.80	4,734	3,725	6.35

[1] Values based on solutions of instances that are feasible in all solution approaches.
[2] Values based on all the instances with feasible solutions for a given approach.

Table 10: Average results of the three MCSRP models with and without the VIs for the instances based on the real case.

Solution method	# Crew	%Feas	%Opt	Avg. time (seconds)	Common feasible instances[1] Avg. upper bound	Common feasible instances[1] Avg. lower bound	Common feasible instances[1] Avg. gap (%)	All feasible instances[2] Avg. upper bound	All feasible instances[2] Avg. lower bound	All feasible instances[2] Avg. gap (%)
MCSRP1	1	42.11	39.47	2,223.74	78,474	75,549	3.14	78,474	75,549	3.14
	3	31.58	28.07	2,559.94	35,929	33,902	5.02	35,454	33,482	4.88
	5	32.46	31.58	2,496.00	35,560	34,669	1.58	35,560	34,669	1.58
MCSRP2	1	42.11	38.60	2,156.08	78,467	75,944	2.10	78,467	75,944	2.10
	3	34.21	28.95	2,534.52	35,929	33,205	6.26	37,113	34,599	5.78
	5	34.21	31.58	2,426.17	35,560	34,669	1.58	38,413	37,568	1.50
MCSRP3	1	42.11	38.60	2,156.10	78,467	75,944	2.10	78,467	75,944	2.10
	3	33.33	29.82	2,532.74	35,929	34,483	3.24	38,069	36,699	3.07
	5	35.09	32.46	2,395.94	35,560	34,669	1.58	37,912	37,088	1.46
MCSRP1 + VIs	1	93.86	68.42	1,264.27	78,467	78,467	0.00	125,474	111,894	5.55
	3	93.86	76.32	1,015.12	35,929	35,929	0.00	69,168	65,841	3.87
	5	89.47	67.54	1,302.04	35,560	35,560	0.00	65,888	59,970	7.60
MCSRP2 + VIs	1	97.37	71.93	1,225.11	78,467	78,467	0.00	125,612	113,517	5.13
	3	94.74	58.77	1,670.53	35,929	35,929	0.00	71,501	63,627	7.36
	5	95.61	52.63	1,873.20	35,560	35,560	0.00	68,479	58,362	10.78
MCSRP3 + VIs	1	100.00	74.56	1,247.62	78,467	78,467	0.00	127,720	115,219	5.26
	3	100.00	55.26	1,884.45	35,929	35,929	0.00	80,824	64,543	10.78
	5	100.00	52.63	2,024.23	35,560	35,560	0.00	72,640	59,176	13.05

[1] Values based on solutions of instances that are feasible in all solution approaches.
[2] Values based on all the instances with feasible solutions for a given approach.

Table 11: Average results of the MCSRP3+VIs strategy for the different instance classes.

Instances	#Crew	#Ins	#Opt	%Opt	Avg. upper bound	Avg. lower bound	Avg. gap (%)	Avg. time (seconds)
L1, L2, L3	1	36	36	100.00	14,121	14,118	0.00	180.65
	3	36	33	91.67	6,708	6,453	0.69	407.86
	5	36	32	88.89	6,114	5,768	1.09	406.77
L4, L5, L6	1	36	36	100.00	11,101	11,095	0.00	298.64
	3	36	31	86.11	4,811	4,669	0.99	533.29
	5	36	31	86.11	4,371	4,178	1.56	626.29
L7, L8, L9	1	36	27	75.00	6,395	4,789	7.80	902.51
	3	36	27	75.00	3,615	2,956	5.62	902.10
	5	36	29	80.56	2,751	2,206	6.44	804.15
L10, L11, L12	1	36	27	75.00	13,389	6,920	13.87	932.17
	3	36	26	72.22	7,114	3,603	14.58	1,094.88
	5	36	26	72.22	5,699	2,747	16.30	1,005.20
CS0	1	6	6	100.00	19,686	19,686	0.00	0.12
	2	6	6	100.00	18,995	18,995	0.00	1.83
	3	6	6	100.00	18,976	18,975	0.00	1.96
CS1, CS2, CS3	1	54	43	79.63	106,250	101,232	2.94	1,125.37
	2	54	29	53.70	69,936	57,229	9.92	2,060.88
	3	54	29	53.70	65,193	53,880	11.83	2,051.85
CS4, CS5, CS6	1	54	36	66.67	161,192	139,821	8.16	1,508.48
	2	54	28	51.85	98,581	76,918	12.84	1,917.19
	3	54	25	46.30	86,049	68,939	15.71	2,221.30

Table 12: Average results of the MCSRP3+VIs* strategy for the different instance classes.

Instances	#Crew	#Ins	#Opt	%Opt	Avg. upper bound	Avg. lower bound	Avg. gap (%)	Avg. time (seconds)
L1, L2, L3	1	36	36	100.00	14,121	14,120	0.00	191.86
	3	36	36	100.00	6,684	6,684	0.00	413.08
	5	36	36	100.00	6,026	6,025	0.00	406.98
L4, L5, L6	1	36	36	100.00	11,101	11,101	0.00	326.91
	3	36	36	100.00	4,811	4,811	0.00	622.01
	5	36	36	100.00	4,361	4,361	0.00	639.57
L7, L8, L9	1	36	27	75.00	6,242	5,103	5.50	903.19
	3	36	31	86.11	3,464	3,197	2.32	904.10
	5	36	30	83.33	2,644	2,315	3.88	888.68
L10, L11, L12	1	36	27	75.00	12,951	8,916	9.24	1,112.49
	3	36	26	72.22	6,325	4,334	10.13	1,106.88
	5	36	26	72.22	4,530	3,207	10.26	1,117.06
CS0	1	6	6	100.00	19,686	19,686	0.00	0.22
	2	6	6	100.00	18,995	18,995	0.00	1.84
	3	6	6	100.00	18,976	18,976	0.00	2.41
CS1, CS2, CS3	1	54	43	79.63	106,142	101,807	2.50	1,292.92
	2	54	40	74.07	63,816	60,840	3.20	2,078.90
	3	54	34	62.96	61,371	57,419	4.69	2,139.12
CS4, CS5, CS6	1	54	37	68.52	158,404	142,114	6.27	1,654.53
	2	54	38	70.37	90,233	83,260	5.62	2,039.23
	3	54	31	57.41	84,047	75,483	7.53	2,259.14

References

Ajam, M., Akbari, V., and Salman, F. S. (2019). Minimizing latency in post-disaster road clearance operations. *European Journal of Operational Research*, 277(3):1098–1112.

Akbari, V. and Salman, F. S. (2017a). Multi-vehicle prize collecting arc routing for connectivity problem. *Computers & Operations Research*, 82:52–68.

Akbari, V. and Salman, F. S. (2017b). Multi-vehicle synchronized arc routing problem to restore post-disaster network connectivity. *European Journal of Operational Research*, 257(2):625–640.

Alem, D., Clark, A., and Moreno, A. (2016). Stochastic network models for logistics planning in disaster relief. *European Journal of Operational Research*, 255(1):187–206.

Aslan, E. and Çelik, M. (2018). Pre-positioning of relief items under road/facility vulnerability with concurrent restoration and relief transportation. *IISE Transactions*, 5854:1–22.

Berktaş, N., Kara, B. Y. Y., Karaşan, O. E., Berktas, N., Kara, B. Y. Y., and Karasan, O. E. (2016). Solution methodologies for debris removal in disaster response. *EURO Journal on Computational Optimization*, 4(3-4):403–445.

Booth, W. (2010). Washington post. Accessed on 20/08/2019.

Bui, Q. T., Deville, Y., and Pham, Q. D. (2016). Exact methods for solving the elementary shortest and longest path problems. *Annals of Operations Research*, 244(2):313–348.

Çelik, M. (2016). Network restoration and recovery in humanitarian operations: Framework, literature review, and research directions. *Surveys in Operations Research and Management Science*, 21(2):47–61.

Çelik, M., Ergun, Ö., and Keskinocak, P. P. (2015). The Post-Disaster Debris Clearance Problem Under Incomplete Information. *Operations Research*, 63(1):65–85.

Dolan, E. D. and Moré, J. J. (2002). Benchmarking optimization software with performance profiles. *Mathematical Programming*, 91(2):201–213.

EM-DAT (2019). The international disaster database. Accessed on 01/06/2019.

Feng, C.-m. and Wang, T.-c. (2003). Highway Emergency Rehabilitation Scheduling in Post-Earthquake 72 Hours. *Journal of the Eastern Asia Society for Transportation Studies*, 5:3276–3285.

Hu, S., Han, C., Dong, Z. S., and Meng, L. (2019). A multi-stage stochastic programming model for relief distribution considering the state of road network. *Transportation Research Part B: Methodological*, 123:64–87.

Hu, Z.-H. and Sheu, J.-B. (2013). Post-disaster debris reverse logistics management under psychological cost minimization. *Transportation Research Part B: Methodological*, 55:118–141.

Irnich, S., Toth, P., and Vigo, D. (2014). Chapter 1: The Family of Vehicle Routing Problems. In Toth, P. and Vigo, D., editors, *Vehicle Routing: Problems, Methods, and Applications*, pages 1–33. SIAM.

Kasaei, M. and Salman, F. S. (2016). Arc routing problems to restore connectivity of a road network. *Transportation Research Part E: Logistics and Transportation Review*, 95:177–206.

Kim, S., Shin, Y., Lee, G. M., and Moon, I. (2018). Network repair crew scheduling for short-term disasters. *Applied Mathematical Modelling*, 64:510–523.

Lorca, Á., Çelik, M., Ergun, Ö., and Keskinocak, P. (2017). An Optimization-Based Decision-Support Tool for Post-Disaster Debris Operations. *Production and Operations Management*, 26(6):1076–1091.

Maya-Duque, P. A., Dolinskaya, I. S., and Sörensen, K. (2016). Network repair crew scheduling and routing for emergency relief distribution problem. *European Journal of Operational Research*, 248(1):272–285.

Moreno, A., Alem, D., and Ferreira, D. (2016). Heuristic approaches for the multiperiod location-transportation problem with reuse of vehicles in emergency logistics. *Computers & Operations Research*, 69:79–96.

Moreno, A., Alem, D., Ferreira, D., and Clark, A. (2018). An effective two-stage stochastic multi-trip location-transportation model with social concerns in relief supply chains. *European Journal of Operational Research*, 269(3):1050–1071.

Moreno, A., Munari, P., and Alem, D. (2019). A branch-and-Benders-cut algorithm for the Crew Scheduling and Routing Problem in road restoration. *European Journal of Operational Research*, 275(1):16–34.

Moreno, A., Munari, P., and Alem, D. (2020). Decomposition-based algorithms for the crew scheduling and routing problem in road restoration. *Computers & Operations Research*, 119:104935.

Morshedlou, N., González, A. D., and Barker, K. (2018). Work crew routing problem for infrastructure network restoration. *Transportation Research Part B: Methodological*, 118:66–89.

OSHA (2019). Flood preparedness and response. *Occupational Safety and Health Administration*. . Accessed on 01/08/2019.

Özdamar, L., Tüzün Aksu, D., and Ergüneş, B. (2014). Coordinating debris cleanup operations in post disaster road networks. *Socio-Economic Planning Sciences*, 48(4):249–262.

Rawls, C. G. and Turnquist, M. a. (2010). Pre-positioning of emergency supplies for disaster response. *Transportation Research Part B: Methodological*, 44(4):521–534.

Rio de Janeiro (2011). Resolução Nº 09/2011 da Assembléia Legislativa. in Portuguese.

Sahin, H., Kara, B. Y., and Karasan, O. E. (2016). Debris removal during disaster response: A case for Turkey. *Socio-Economic Planning Sciences*, 53:49–59.

Sanci, E. and Daskin, M. S. (2019). Integrating location and network restoration decisions in relief networks under uncertainty. *European Journal of Operational Research*, 279(2):335–350.

Shin, Y., Kim, S., and Moon, I. (2019). Integrated optimal scheduling of repair crew and relief vehicle after disaster. *Computers and Operations Research*, 105:237–247.

Taillard, E. D. (1999). A heuristic column generation method for the heterogeneous fleet VRP. *RAIRO - Operations Research*, 33(1):1–14.

Tang, C.-H., Yan, S., and Chang, C.-W. (2009). Short-term work team scheduling models for effective road repair and management. *Transportation Planning and Technology*, 32(3):289–311.

Tuzun Aksu, D. and Ozdamar, L. (2014). A mathematical model for post-disaster road restoration: Enabling accessibility and evacuation. *Transportation Research Part E: Logistics and Transportation Review*, 61:56–67.

Tzeng, G.-H., Chen, Y.-W., and Lin, C.-Y. (2000). Fuzzy Multi-objective Reconstruction Plan for Post-earthquake Road-network by Genetic Algorithm. *Research and Practice in Multiple Criteria Decision Making*, 487:510–528.

Van Wassenhove, L., Martinez, A., and Stapleton, O. (2010). Insead humanitarian research group. Accessed on 20/08/2019.

Xu, B. and Song, Y. (2015). An Ant Colony-based Heuristic Algorithm for Joint Scheduling of Post-earthquake Road Repair and Relief Distribution. *TELKOMNIKA (Telecommunication Computing Electronics and Control)*, 13(2):632.

Yan, S., Chu, J. C., and Shih, Y.-L. (2014). Optimal scheduling for highway emergency repairs under large-scale supply-demand perturbations. *IEEE Transactions on Intelligent Transportation Systems*, 15(6):2378–2393.

Yan, S. and Shih, Y.-L. (2007). A time-space network model for work team scheduling after a major disaster. *Journal of the Chinese Institute of Engineers*, 30(1):63–75.

Yan, S. and Shih, Y.-L. (2009). Optimal scheduling of emergency roadway repair and subsequent relief distribution. *Computers and Operations Research*, 36(6):2049–2065.

Yan, S. and Shih, Y.-L. (2012). An ant colony system-based hybrid algorithm for an emergency roadway repair time-space network flow problem. *Transportmetrica*, 8(5):361–386.